



Asynchronous Federated Learning: A Scalable Approach for Decentralized Machine Learning

Ali Forootani*, Senior Member, IEEE ^a, Raffaele Iervolino, Senior Member, IEEE ^b



^a*Helmholtz Centre for Environmental Research - UFZ, Permoserstraße 15, 04318 Leipzig, Germany.*

^b*Department of Electrical Engineering and Information Technology, University of Naples, 80125 Napoli, Italy.*

Abstract

Federated Learning (FL) has emerged as a powerful paradigm for decentralized machine learning, enabling collaborative model training across diverse clients without sharing raw data. However, traditional FL approaches often face limitations in scalability and efficiency due to their reliance on synchronous client updates, which can result in significant delays and increased communication overhead, particularly in heterogeneous and dynamic environments. To address these challenges in this paper, we propose an Asynchronous Federated Learning (AFL) algorithm, which allows clients to update the global model independently and asynchronously.

Our key contributions include a comprehensive convergence analysis of AFL in the presence of client delays and model staleness. By leveraging martingale difference sequence theory and variance bounds, we ensure robust convergence despite asynchronous updates. Assuming μ -strongly convex local objective functions, we establish bounds on gradient variance under random client sampling and derive a recursion formula quantifying the impact of client delays on convergence. Furthermore, we demonstrate the practical applicability of AFL by training a decentralized Long Short-Term Memory (LSTM)-based deep learning model on the CMIP6 climate dataset, effectively handling non-IID and geographically distributed data.

Email addresses: ali.forootani@ufz.de-aliforootani@ieee.org (Ali Forootani*, Senior Member, IEEE ) , rafierv@unina.it (Raffaele Iervolino, Senior Member, IEEE )

The proposed AFL algorithm addresses key limitations of traditional FL methods, such as inefficiency due to global synchronization and susceptibility to client drift. It enhances scalability, robustness, and efficiency in real-world settings with heterogeneous client populations and dynamic network conditions. Our results underscore the potential of AFL to drive advancements in distributed learning systems, particularly for large-scale, privacy-preserving applications in resource-constrained environments.

Keywords: Federated Learning, Stochastic Gradient Descent, Client Drifts, Asynchronous Federated Learning,

1. Introduction

Federated Learning (FL) is a distributed machine learning approach that enables multiple devices or nodes (often called “clients”) to collaboratively train a shared model while keeping their data locally, without centralizing it Li et al. [1]. In contrast to traditional machine learning methods that require data to be stored in a central server, FL enhances data privacy and security by ensuring that raw data never leaves the client devices Zhang et al. [2]. This paradigm is particularly valuable in applications where data privacy is a concern, such as healthcare Antunes et al. [3], finance Wen et al. [4], and IoT (Internet of Things) systems Nguyen et al. [5].

FL encompasses two primary strategies for training models across multiple clients: parallel FL (PFL) and sequential FL (SFL). In PFL, clients perform local training on their respective data in a synchronized manner, where models are periodically aggregated across clients, as exemplified by Federated Averaging (FedAvg) McMahan et al. [6]. This approach allows multiple clients to simultaneously contribute updates to the central model, promoting efficient use of parallel processing capabilities. Alternatively, SFL adopts a different training mechanism. Here, model updates are passed sequentially between clients, as seen in Cyclic Weight Transfer (CWT) Chang et al. [7]. This method enables model knowledge transfer by having each client build on the model updates from the previous client, which can be advantageous in certain applications but also introduces latency due to the sequential nature of training. Despite their distinct workflows, both PFL and SFL encounter a challenge commonly referred to as “client drift” Karimireddy et al. [8]. This phenomenon arises when client updates, particularly in heterogeneous data environments, diverge significantly from each other. Such divergence can impact convergence

and reduce model accuracy, especially when client data distributions vary widely.

The convergence of PFL and its optimization via methods like Random Reshuffling Stochastic Gradient Descent (SGD-RR) has been a focus of extensive research, especially in the context of addressing challenges in federated settings. Studies on data heterogeneity—where clients have diverse, non-iid data distributions—have proposed techniques to stabilize convergence and reduce client drift, such as through adaptive algorithms and regularization methods Li et al. [9], Khaled et al. [10], Karimireddy et al. [8], Koloskova et al. [11], Woodworth et al. [12]. System heterogeneity, which refers to variations in client capabilities and resource constraints, has also been a critical area of research, with strategies developed to handle differences in client availability and computation speeds Wang et al. [13]. Moreover, approaches to handle partial client participation, where only a subset of clients are selected for training in each round, have aimed to balance efficiency with convergence accuracy Li et al. [9], Yang et al. [14], Wang and Ji [15]. Additionally, other variants of PFL incorporate adaptive mechanisms that can respond to fluctuating client conditions and data distributions, further refining the robustness and scalability of federated systems Karimireddy et al. [8], Reddi et al. [16].

While Random Reshuffling Stochastic Gradient Descent (SGD-RR) has been shown to improve convergence stability over standard SGD by sampling data without replacement, it is not without limitations. The upper bounds established for SGD-RR Gürbüzbalaban et al. [17], Haochen and Sra [18], Nagaraj et al. [19], Ahn et al. [20], Mishchenko et al. [21] suggest that the algorithm can achieve improved convergence rates, especially under smoothness and convexity assumptions. However, these bounds often rely on idealized assumptions that may not hold in real-world applications, such as uniformity across reshuffling cycles or independence between batches. This limits the practical applicability of these theoretical guarantees, particularly in scenarios with non-iid or highly heterogeneous data distributions.

Furthermore, while lower bounds Safran and Shamir [22, 23], Rajput et al. [24], Cha et al. [25] have been shown to match the upper bounds in some cases, especially in the recent work by Cha et al. [25] that aligns with Mishchenko et al. [21], these analyses still assume a certain regularity in data and task structure that might not be representative of complex data landscapes. For example, in high-variance settings or non-convex optimization problems, SGD-RR can suffer from convergence issues similar to those faced by standard SGD, as it does not inherently address gradient noise or data

imbalance. Additionally, SGD-RR may increase computational overhead due to the need for data reshuffling, which can be computationally costly in large datasets or distributed environments. Consequently, while SGD-RR represents a step forward in optimization, more adaptive and robust methods are needed to handle the diversity of practical applications beyond what current theoretical bounds suggest.

Recently, shuffling-based methods have been extended to FL, with studies exploring their convergence properties in this context Mishchenko et al. [26], Yun et al. [27], Cho et al. [28]. These methods, inspired by the success of shuffling in traditional machine learning, aim to improve the efficiency and robustness of FL by addressing challenges related to data heterogeneity and client participation. In particular, Cho et al. [28] analyzed the convergence behavior of FL with cyclic client participation, providing insights into how different client participation schemes—whether parallel or sequential—affect the overall model convergence. The work highlights that both PFL and SFL can be viewed as specific instances of this cyclic participation framework, where clients update the global model in a structured, repeated manner. This approach not only clarifies the relationship between these methods but also introduces a more generalized framework that can potentially improve convergence rates by optimizing the order and frequency of client participation. However, despite these advancements, challenges remain in handling extremely heterogeneous data across clients, and further research is needed to refine these methods for large-scale and highly variable federated settings.

AFL also

1.1. Motivation

Asynchronous FL (AFL) is particularly crucial for overcoming the limitations of traditional federated learning methods, especially in scenarios involving heterogeneous and large-scale client populations Chen et al. [29]. In conventional FL, synchronous methods—such as Federated Averaging (FedAvg)—require all participating clients to update their models and synchronize their weights with the central server at the same time. This synchronization can be inefficient, especially when dealing with clients that have varying computational resources, data distributions, and network conditions. In such settings, waiting for all clients to finish their updates can lead to significant delays and increased communication costs, particularly when clients are highly heterogeneous or when network conditions are unstable.

In contrast, AFL allows each client to send updates to the server asynchronously, as soon as they finish their local training. This flexibility alleviates the bottleneck created by the need for global synchronization, enabling the server to aggregate and update the model more frequently, which can lead to faster convergence. Moreover, this approach is more scalable because it reduces the dependency on a synchronized round of communication between all clients, making it well-suited for large-scale federated learning systems.

Additionally, AFL helps mitigate the issue of “client drift”, where updates from heterogeneous clients with varying data distributions may diverge from the optimal direction in synchronized settings. By enabling more frequent updates from each client, AFL can smooth out these fluctuations and promote more stable convergence. Furthermore, clients with different computational capabilities can participate without causing delays for others, as slower clients are not required to synchronize with faster ones. This characteristic is especially important in federated environments where devices with varying hardware, such as mobile phones or IoT devices, are involved.

In essence, AFL offers significant advantages in terms of efficiency, scalability, and robustness, making it a powerful method for federated systems that need to accommodate large, diverse, and dynamically changing populations of clients. It is especially beneficial in real-world applications where client heterogeneity, network instability, and varying resource availability are common challenges. In this regard we further extend the early results on AFL reported in Chen et al. [29], Leconte et al. [30] by providing comprehensive convergence analysis and new results on client drifts, dynamic learning rates and random selection of clients in training rounds.

1.2. Contributions

In this work, we propose an AFL algorithm, aiming to address convergence challenges inherent in distributed, asynchronous setups. Key contributions of our approach are summarized below:

(i) We conduct a comprehensive convergence analysis for AFL, where updates from local clients are asynchronously applied to the global model. This setup inherently introduces delays and model staleness, which we address by building on theoretical results related to martingale difference sequences and sampling variance bounds. In particular, the extended bound on the variance of a martingale difference sequence ensures that the cumulative variance grows linearly with the number of terms, each controlled by a bounded variance δ^2 . This result allows us to manage the additional variance introduced

by asynchronous updates and provides a key foundation for the stability of AFL.

(ii) Our convergence results are established under the assumption that each client’s local objective function is strongly convex. This assumption enables us to leverage properties of convex functions, particularly when combining them with the quadratic term in the local objectives.

(iii) We derive specific bounds on the variance when we sampling clients without replacement, which are critical in federated settings where data may be non-IID and limited per client. We establish that the variance of the sample mean diminishes as the sample size increases, supporting the accuracy of gradient estimations in each client’s local updates. Furthermore, we extend this analysis to address sequential partial participation of the clients and derive a bound on the cumulative variance for multi-step updates, allowing us to control for delayed information in asynchronous participation.

(iv) Finally, we establish a recursion formula for the AFL algorithm in the strongly convex setting. Through this recursion, we demonstrate how the delay τ_c of each client’s update affects the overall convergence. We show that despite potential staleness in gradient updates, our algorithm remains robust due to the strongly convex nature of the local objectives and the bounded variance of updates, ultimately achieving reliable convergence.

(v) In the simulation phase, we employed the asynchronous federated learning (AFL) algorithm to train a decentralized Long Short-Term Memory (LSTM)-based deep learning model on the climate dataset. This approach enabled multiple clients, each representing a distinct geographic region, to independently train local models on regional climate data while asynchronously sharing updates with a central server. By leveraging AFL, we effectively utilized distributed data without centralization, ensuring privacy and computational efficiency, while accounting for client-specific conditions such as delays and heterogeneous data distributions.

This paper is organized as follows: In section 2 preliminaries are given. Problem formulation will be discussed in section 3. To prove the convergence of the AFL algorithm we need some theoretical results that will be provided in section 4. In section 5 we prove the convergence of our AFL algorithm. Simulation and the case study will be discussed in section 6. Finally section 7 concludes the paper.

2. Preliminaries and main assumptions

In the following, we provide some preliminaries on AFL, highlighting its distinct approach in comparison to traditional PFL.

Notation. As done in Cha et al. [25], we use \gtrsim to mean “greater than” up to some absolute constants and slowly growing factors, like polylogarithmic terms. Similarly, \lesssim denotes “less than” up to these constants and slower-growing factors, and \asymp represents “approximately equal” up to the same constants and polylogarithmic factors.

We denote by $\|\cdot\|$ the standard Euclidean norm, applicable to both vectors and matrices. The constant μ indicates the level of strong convexity, while σ provides an upper bound on the variance of the stochastic gradients for each client involved in the AFL. The number of clients is represented by C , with c indexing a specific client, and J indicates the number of clients actively participating in training. The number of training rounds is denoted by \mathcal{J} , with j representing the index of a particular round. The number of local update steps is given by I , and i indexes a specific local step. We define λ as the learning rate or step size. The effective learning rate, $\tilde{\lambda}$, is defined as $\tilde{\lambda} = \lambda CI$ in AFL. The symbol ψ represents a permutation of client indices, written as $\{\psi_1, \psi_2, \dots, \psi_C\}$ over the set $\{1, 2, \dots, C\}$. The global objective function is denoted by F , while F_c refers to the local objective function for client c . The global model parameters at the j -th training round are given by $\mathbf{x}^{(j)}$, and $\mathbf{x}_{c,i}^{(j)}$ denotes the local model parameters of client c after i local updates within the j -th round.

Stochastic gradients for client ψ_c 's objective F_{ψ_c} , with respect to $\mathbf{x}_{c,i}^{(j)}$, are represented by $\mathbf{q}_{\psi_c,i}^{(j)}$, where $\mathbf{q}_{\psi_c,i}^{(j)} := \nabla f_{\psi_c}(\mathbf{x}_{c,i}^{(j)}; \xi)$. The variance of a random variable \mathbf{x} can be expressed using the following identity:

$$\mathbb{E} [\|\mathbf{x} - \mathbb{E}[\mathbf{x}]\|^2] = \mathbb{E} [\|\mathbf{x}\|^2] - \|\mathbb{E}[\mathbf{x}]\|^2. \quad (1)$$

This relationship can also be applied to a finite collection of vectors. Specifically, for vectors $\mathbf{x}_1, \dots, \mathbf{x}_m \in \mathbb{R}^d$, the variance is given by:

$$\frac{1}{m} \sum_{k=1}^m \|\mathbf{x}_k - \bar{\mathbf{x}}\|^2 = \frac{1}{m} \sum_{k=1}^m \|\mathbf{x}_k\|^2 - \left\| \frac{1}{m} \sum_{k=1}^m \mathbf{x}_k \right\|^2, \quad (2)$$

where the mean vector is defined as $\bar{\mathbf{x}} = \frac{1}{m} \sum_{k=1}^m \mathbf{x}_k$. This equation illustrates how the variance can be decomposed into the average of squared norms and the squared norm of the mean.

Let h be any convex function, and consider vectors $\mathbf{x}_1, \dots, \mathbf{x}_m$. The Jensen's Inequality states that:

$$h\left(\frac{1}{m}\sum_{k=1}^m\mathbf{x}_k\right)\leq\frac{1}{m}\sum_{k=1}^mh(\mathbf{x}_k). \quad (3)$$

A notable application arises when $h(\mathbf{x}) = \|\mathbf{x}\|^2$. Substituting this specific convex function, we obtain:

$$\left\|\frac{1}{m}\sum_{k=1}^m\mathbf{x}_k\right\|^2\leq\frac{1}{m}\sum_{k=1}^m\|\mathbf{x}_k\|^2. \quad (4)$$

This result demonstrates how Jensen's inequality relates to the squared norm, bounding the norm of the mean by the mean of the norms.

A sequence of random variables $\{X_m\}_{m=1}^\infty$ is called a martingale with respect to a filtration (a growing collection of information) $\{\mathcal{F}_m\}_{m=1}^\infty$ if it satisfies the following properties: (i) Adapted-ness: Each random variable X_m is \mathcal{F}_m -measurable, meaning it is based on the information available up to time m . (ii) Integrability: The expected value of each random variable is finite:

$$\mathbb{E}[|X_m|] < \infty \quad \text{for all } m.$$

(iii) Martingale Property: The expected value of the next observation, given all prior observations, is equal to the current observation:

$$\mathbb{E}[X_{m+1} \mid \mathcal{F}_m] = X_m \quad \text{for all } m.$$

Bregman Divergence for a function f and points \mathbf{x} and \mathbf{y} is defined by

$$D_f(\mathbf{x}, \mathbf{y}) := f(\mathbf{x}) - f(\mathbf{y}) - \langle \nabla f(\mathbf{y}), \mathbf{x} - \mathbf{y} \rangle.$$

This divergence measure is always non-negative when f is convex. Moreover, if f is both convex and L -smooth (for the definition of convexity, see Boyd and Vandenberghe [31]), the Bregman divergence satisfies the inequality

$$D_f(\mathbf{x}, \mathbf{y}) \geq \frac{1}{2L} \|\nabla f(\mathbf{x}) - \nabla f(\mathbf{y})\|^2. \quad (5)$$

This lower bound captures the relationship between the Bregman divergence and the gradient differences under these conditions.

2.1. Assumptions

We provide the main assumptions that are required in this article for the AFL convergence analysis.

Assumption 1. *Each function \mathcal{F}_c , representing the local objective for $c \in \{1, 2, \dots, C\}$, is assumed to be L -smooth. This property implies the existence of a constant $L > 0$ such that, for any pair of points \mathbf{x} and \mathbf{y} in \mathbb{R}^d ,*

$$\|\nabla\mathcal{F}_c(\mathbf{x}) - \nabla\mathcal{F}_c(\mathbf{y})\| \leq L \|\mathbf{x} - \mathbf{y}\|.$$

Here, L serves as the smoothness constant, providing an upper bound on the rate of change of the gradient of \mathcal{F}_c .

The algorithms outlined in Algorithm 1 employ Stochastic Gradient Descent (SGD) with data samples drawn without replacement at each client.

Assumption 2. *We assume that the variance of the stochastic gradient in AFL for any given client is uniformly bounded. Specifically, for all $c \in \{1, 2, \dots, C\}$, the following inequality holds:*

$$\mathbb{E}_{\xi \sim \mathcal{D}_c} [\|\nabla f_c(\mathbf{x}; \xi) - \nabla\mathcal{F}_c(\mathbf{x})\|^2 \mid \mathbf{x}] \leq \delta^2,$$

where \mathcal{D}_c represents the data distribution for client c .

Assumption 3a. *We posit that the gradients of the local objective functions do not significantly deviate from the gradient of the global objective function across the optimization space. Specifically, there exist constants ϕ^2 and β^2 such that the following inequality holds:*

$$\frac{1}{C} \sum_{c=1}^C \|\nabla\mathcal{F}_c(\mathbf{x}) - \nabla\mathcal{F}(\mathbf{x})\|^2 \leq \phi^2 \|\nabla\mathcal{F}(\mathbf{x})\|^2 + \beta^2.$$

Here, $\nabla\mathcal{F}_c(\mathbf{x})$ denotes the gradient of the local objective function for each client c , while $\nabla\mathcal{F}(\mathbf{x})$ refers to the gradient of the global objective function. The constants ϕ and β quantify the degree of heterogeneity among clients; when $\phi = 0$ and $\beta = 0$, all local objectives coincide exactly with the global objective.

Assumption 3b. At the global minimizer \mathbf{x}^* , we assume that the gradients of the local objective functions do not vary widely from each other. In particular, there exists a constant β_*^2 such that:

$$\frac{1}{C} \sum_{c=1}^C \|\nabla \mathcal{F}_c(\mathbf{x}^*)\|^2 = \beta_*^2,$$

where β_* quantifies the degree of gradient similarity at \mathbf{x}^* , the minimizer of the global objective $F(\mathbf{x})$.

Assumption 3c. A function $h : \mathbb{R}^d \rightarrow \mathbb{R}$ is called μ -strongly convex if and only if it can be expressed as the sum of a convex function $q : \mathbb{R}^d \rightarrow \mathbb{R}$ and a quadratic term, specifically:

$$h(\mathbf{x}) = q(\mathbf{x}) + \frac{\mu}{2} \|\mathbf{x}\|^2,$$

where $\mu > 0$ represents the strong convexity parameter.

3. Problem Formulation

The goal of the FL algorithm is to minimize a global objective function defined as follows:

$$\min_{\mathbf{x} \in \mathbb{R}^d} \left\{ F(\mathbf{x}) := \frac{1}{C} \sum_{c=1}^C (\mathcal{F}_c(\mathbf{x}) := \mathbb{E}_{\xi \sim \mathcal{D}_c} [f_c(\mathbf{x}; \xi)]) \right\},$$

where \mathcal{F}_c , f_c , and \mathcal{D}_c are the local objective function, the loss function, and the dataset associated with client c , respectively ($c \in [C]$).

If \mathcal{D}_c consists of a finite set of data samples $\{\xi_c^j : j \in [|\mathcal{D}_c|]\}$, then the local objective function can be equivalently written as:

$$\mathcal{F}_c(\mathbf{x}) = \frac{1}{|\mathcal{D}_c|} \sum_{j=1}^{|\mathcal{D}_c|} f_c(\mathbf{x}; \xi_c^j).$$

Each client c performs updates independently and asynchronously, with an associated update delay τ_c , representing the time gap between when a client computes its gradient and when the global model is updated with that gradient.

In each training round, the client indices $\psi_1, \psi_2, \dots, \psi_C$ are randomly selected without replacement from $\{1, 2, \dots, C\}$. The steps for each selected client ψ_c are as follows:

1. Initialize its model using the most recent global parameters, $\mathbf{x}^{(j-\tau_c)}$, where τ_c is the delay in receiving the global model.
2. Perform I iterations of local updates using its local dataset, with the parameters after the i -th update denoted as $\mathbf{x}_{c,i}^{(j)}$.
3. Upon completing local training, send the final parameters $\mathbf{x}_{c,I}^{(j)}$ to the central server.

The global model $\mathbf{x}^{(j)}$ is updated asynchronously as client updates are received.

The update rule for AFL using Stochastic Gradient Descent (SGD) for local updates is:

$$\text{Local update: } \mathbf{x}_{c,i+1}^{(j)} = \mathbf{x}_{c,i}^{(j)} - \lambda \mathbf{q}_{c,i}^{(j)},$$

with the initialization:

$$\mathbf{x}_{c,0}^{(j)} = \mathbf{x}^{(j-\tau_c)},$$

where $\mathbf{q}_{c,i}^{(j)} := \nabla f_{\psi_c}(\mathbf{x}_{c,i}^{(j)}; \xi)$ denotes the stochastic gradient of the local objective function F_{ψ_c} with respect to the local parameters $\mathbf{x}_{c,i}^{(j)}$.

The global model is updated after receiving the updated parameters from all clients as follows:

$$\text{Global update: } \mathbf{x}^{(j+1)} = \text{Aggregate}(\{\mathbf{x}_{c,I}^{(j-\tau_c)} : c \in [C]\}).$$

This iterative procedure continues, with the global model being updated asynchronously as clients send their local updates. The complete procedure is detailed in Algorithm 1.

where $\mathbf{q}_{c,i}^{(j)} := \nabla q_c(\mathbf{x}_{c,i}^{(j)}; \xi)$ is the stochastic gradient of \mathcal{F}_c with respect to parameters $\mathbf{x}_{c,i}^{(j)}$ and λ denotes the learning rate. The aggregation function may take various forms, such as averaging or weighted averaging, based on the client contributions.

Assumption 3d. *The staleness τ_c is bounded by τ_{\max} :*

$$\tau_c \leq \tau_{\max}.$$

Algorithm 1: AFL update rule with participation of all clients in the training loop

Input: Global model parameters $\mathbf{x}^{(j-\tau_c)}$, local data for each client

Output: Updated global model $\mathbf{x}^{(j+1)}$

- 1 **for** each client $c \in [C]$, **do**
- 2 **for** $i = 0, 1, \dots, I - 1$ **do**
- 3 **Local update:** $\mathbf{x}_{c,i+1}^{(j)} = \mathbf{x}_{c,i}^{(j)} - \lambda \mathbf{q}_{c,i}^{(j)}$;
- 4 **Initialization:** $\mathbf{x}_{c,0}^{(j)} = \mathbf{x}^{(j-\tau_c)}$;
- 5 **Send updated parameters:** $\mathbf{x}_{c,I}^{(j)}$;
- 6 **Global model update:** Upon receiving updated parameters, update the global model as follows:

$$\mathbf{x}^{(j+1)} = \text{Aggregate}(\{\mathbf{x}_{c,I}^{(j-\tau_c)} : c \in [C]\}).$$

4. Theoretical requisite for convergence analysis

In this section, we provide theoretical results that are needed for driving the convergence of AFL. In the next Lemma, we give an extended version of results reported in Karimireddy et al. [8] to establish a bound on the variance of the sum of a martingale difference sequence, showing that the cumulative variance grows linearly with the number of terms in the sequence, each bounded by δ^2 .

Lemma 1. *Let $\{\xi_k\}_{k=1}^m$ be a sequence of random variables, and let $\{\mathbf{x}_k\}_{k=1}^m$ be a sequence of random vectors where each $\mathbf{x}_k \in \mathbb{R}^d$ is determined by $\xi_k, \xi_{k-1}, \dots, \xi_1$. Assume that the conditional expectation $\mathbb{E}_{\xi_k}[\mathbf{x}_k \mid \xi_{k-1}, \dots, \xi_1] = \mathbf{e}_k$ holds for all k , meaning that the sequence $\{\mathbf{x}_k - \mathbf{e}_k\}$ is a martingale difference sequence with respect to $\{\xi_k\}$. Furthermore, suppose that the conditional variance satisfies $\mathbb{E}_{\xi_k}[\|\mathbf{x}_k - \mathbf{e}_k\|^2 \mid \xi_{k-1}, \dots, \xi_1] \leq \delta^2$ for all k . Then, the following inequality holds:*

$$\mathbb{E} \left[\left\| \sum_{k=1}^m (\mathbf{x}_k - \mathbf{e}_k) \right\|^2 \right] = \sum_{k=1}^m \mathbb{E} [\|\mathbf{x}_k - \mathbf{e}_k\|^2] \leq m\delta^2.$$

Proof. The term inside the expectation is the squared norm of the sum:

$$\left\| \sum_{k=1}^m (\mathbf{x}_k - \mathbf{e}_k) \right\|^2.$$

This norm can be expanded as an inner product:

$$\left\| \sum_{k=1}^m (\mathbf{x}_k - \mathbf{e}_k) \right\|^2 = \left(\sum_{k=1}^m (\mathbf{x}_k - \mathbf{e}_k) \right)^\top \left(\sum_{k=1}^m (\mathbf{x}_k - \mathbf{e}_k) \right).$$

We can expand this product by distributing over all terms:

$$\begin{aligned} & \left(\sum_{k=1}^m (\mathbf{x}_k - \mathbf{e}_k) \right)^\top \left(\sum_{k=1}^m (\mathbf{x}_k - \mathbf{e}_k) \right) \\ &= \sum_{k=1}^m \|\mathbf{x}_k - \mathbf{e}_k\|^2 + 2 \sum_{1 \leq k < j \leq m} (\mathbf{x}_k - \mathbf{e}_k)^\top (\mathbf{x}_j - \mathbf{e}_j). \end{aligned} \quad (6)$$

This expansion consists of two parts: (i) The sum of squared norms of each $(\mathbf{x}_k - \mathbf{e}_k)$, which gives terms like $\|\mathbf{x}_k - \mathbf{e}_k\|^2$. (ii) Cross terms for $k \neq j$, each of the form $(\mathbf{x}_k - \mathbf{e}_k)^\top (\mathbf{x}_j - \mathbf{e}_j)$. Thus,

$$\begin{aligned} \left\| \sum_{k=1}^m (\mathbf{x}_k - \mathbf{e}_k) \right\|^2 &= \sum_{k=1}^m \|\mathbf{x}_k - \mathbf{e}_k\|^2 \\ &\quad + 2 \sum_{1 \leq k < j \leq m} (\mathbf{x}_k - \mathbf{e}_k)^\top (\mathbf{x}_j - \mathbf{e}_j). \end{aligned}$$

Now we take the expectation of both sides:

$$\begin{aligned} \mathbb{E} \left[\left\| \sum_{k=1}^m (\mathbf{x}_k - \mathbf{e}_k) \right\|^2 \right] &= \mathbb{E} \left[\sum_{k=1}^m \|\mathbf{x}_k - \mathbf{e}_k\|^2 \right] \\ &\quad + 2 \mathbb{E} \left[\sum_{1 \leq k < j \leq m} (\mathbf{x}_k - \mathbf{e}_k)^\top (\mathbf{x}_j - \mathbf{e}_j) \right]. \end{aligned} \quad (7)$$

Since $\{\mathbf{x}_k - \mathbf{e}_k\}$ is a *martingale difference sequence*, the cross terms $\mathbb{E}[(\mathbf{x}_k - \mathbf{e}_k)^\top (\mathbf{x}_j - \mathbf{e}_j)] = 0$ for $k \neq j$. This is because the martingale property implies that $(\mathbf{x}_k - \mathbf{e}_k)$ is uncorrelated with $(\mathbf{x}_j - \mathbf{e}_j)$ for $j > k$, meaning:

$$\mathbb{E}[(\mathbf{x}_k - \mathbf{e}_k)^\top (\mathbf{x}_j - \mathbf{e}_j)] = 0.$$

More specifically, by definition, a sequence $\{Y_i\}$ is a martingale difference sequence with respect to a filtration $\{F_i\}$ if: $\mathbb{E}[Y_i | F_{i-1}] = 0$ for all i . In this context, we set $Y_i = \mathbf{x}_i - \mathbf{e}_i$ and $F_i = \delta(\xi_1, \dots, \xi_i)$, the δ -algebra generated by $\{\xi_1, \dots, \xi_i\}$. Thus, the martingale difference property means: $\mathbb{E}[\mathbf{x}_i - \mathbf{e}_i | \xi_{i-1}, \dots, \xi_1] = 0$.

Now, if $i < j$, then by the martingale difference property, $\mathbf{x}_j - \mathbf{e}_j$ is orthogonal (has zero expectation when conditioned on) any information up to ξ_i , because: $\mathbb{E}[(\mathbf{x}_j - \mathbf{e}_j) | \xi_i, \dots, \xi_1] = 0$.

For any two indices $i < j$, we can write the cross-term as:

$$\mathbb{E}[(\mathbf{x}_i - \mathbf{e}_i)^\top (\mathbf{x}_j - \mathbf{e}_j)] = \mathbb{E}[(\mathbf{x}_i - \mathbf{e}_i)^\top \mathbb{E}[(\mathbf{x}_j - \mathbf{e}_j) | \xi_i, \dots, \xi_1]].$$

By the martingale difference property, the inner expectation $\mathbb{E}[(\mathbf{x}_j - \mathbf{e}_j) | \xi_i, \dots, \xi_1] = 0$, which implies:

$$\mathbb{E}[(\mathbf{x}_i - \mathbf{e}_i)^\top (\mathbf{x}_j - \mathbf{e}_j)] = \mathbb{E}[(\mathbf{x}_i - \mathbf{e}_i)^\top \cdot 0] = 0.$$

This shows that the cross-term $(\mathbf{x}_i - \mathbf{e}_i)^\top (\mathbf{x}_j - \mathbf{e}_j)$ contributes zero to the overall sum, which simplifies the expression. In summary, the martingale difference property ensures that $\mathbf{x}_j - \mathbf{e}_j$ has zero expectation when conditioned on $\{\xi_1, \dots, \xi_i\}$ for $i < j$, making all cross-terms zero and allowing the sum of squared norms to simplify.

Thus, the cross-term expectation sums to zero:

$$\mathbb{E}\left[\sum_{1 \leq i < j \leq m} (\mathbf{x}_i - \mathbf{e}_i)^\top (\mathbf{x}_j - \mathbf{e}_j)\right] = 0.$$

This leaves us with:

$$\mathbb{E}\left[\left\|\sum_{i=1}^m (\mathbf{x}_i - \mathbf{e}_i)\right\|^2\right] = \sum_{i=1}^m \mathbb{E}[\|\mathbf{x}_i - \mathbf{e}_i\|^2].$$

And, since each variance term is bounded by δ^2 :

$$\mathbb{E}\left[\left\|\sum_{i=1}^m (\mathbf{x}_i - \mathbf{e}_i)\right\|^2\right] \leq m\delta^2.$$

This completes the breakdown of the lemma. The key step here is that the martingale difference property ensures the cross terms are zero, allowing us to focus only on the sum of variances of individual terms.

□

The next lemma we discuss the properties of convex functions that we use in this article which is originally reported in Karimireddy et al. [8] and we provide different proof for it.

Lemma 2 (Karimireddy et al. [8]). *For a L -smooth and μ -strongly convex function h , we have*

$$\begin{aligned} \langle \nabla h(\mathbf{x}), \mathbf{z} - \mathbf{y} \rangle &\geq h(\mathbf{z}) - h(\mathbf{y}) + \frac{\mu}{4} \|\mathbf{y} - \mathbf{z}\|^2 - L \|\mathbf{z} - \mathbf{x}\|^2, \\ &\forall \mathbf{x}, \mathbf{y}, \mathbf{z} \in \text{domain}(h). \end{aligned} \quad (8)$$

Proof. Since h is L -smooth, for any \mathbf{x} , and \mathbf{z} in the domain of h , we have: $h(\mathbf{z}) \leq h(\mathbf{x}) + \langle \nabla h(\mathbf{x}), \mathbf{z} - \mathbf{x} \rangle + \frac{L}{2} \|\mathbf{z} - \mathbf{x}\|^2$. Rearranging gives:

$$\langle \nabla h(\mathbf{x}), \mathbf{z} - \mathbf{x} \rangle \geq h(\mathbf{z}) - h(\mathbf{x}) - \frac{L}{2} \|\mathbf{z} - \mathbf{x}\|^2.$$

Since h is μ -strongly convex, we have:

$$h(\mathbf{y}) \geq h(\mathbf{x}) + \langle \nabla h(\mathbf{x}), \mathbf{y} - \mathbf{x} \rangle + \frac{\mu}{2} \|\mathbf{y} - \mathbf{x}\|^2.$$

Rearranging gives:

$$\langle \nabla h(\mathbf{x}), \mathbf{y} - \mathbf{x} \rangle \leq h(\mathbf{y}) - h(\mathbf{x}) - \frac{\mu}{2} \|\mathbf{y} - \mathbf{x}\|^2.$$

We can express $\langle \nabla h(\mathbf{x}), \mathbf{z} - \mathbf{y} \rangle$ as:

$$\langle \nabla h(\mathbf{x}), \mathbf{z} - \mathbf{y} \rangle = \langle \nabla h(\mathbf{x}), \mathbf{z} - \mathbf{x} \rangle + \langle \nabla h(\mathbf{x}), \mathbf{x} - \mathbf{y} \rangle.$$

Substituting the bounds from Steps (4) and (4):

$$\begin{aligned} \langle \nabla h(\mathbf{x}), \mathbf{z} - \mathbf{y} \rangle &\geq \left(h(\mathbf{z}) - h(\mathbf{x}) - \frac{L}{2} \|\mathbf{z} - \mathbf{x}\|^2 \right) \\ &\quad + \left(h(\mathbf{x}) - h(\mathbf{y}) + \frac{\mu}{2} \|\mathbf{y} - \mathbf{x}\|^2 \right). \end{aligned}$$

This simplifies to:

$$\langle \nabla h(\mathbf{x}), \mathbf{z} - \mathbf{y} \rangle \geq h(\mathbf{z}) - h(\mathbf{y}) + \frac{\mu}{2} \|\mathbf{y} - \mathbf{x}\|^2 - \frac{L}{2} \|\mathbf{z} - \mathbf{x}\|^2.$$

Applying Jensen's inequality:

$$\|\mathbf{y} - \mathbf{z}\|^2 \leq 2\|\mathbf{x} - \mathbf{z}\|^2 + 2\|\mathbf{x} - \mathbf{y}\|^2.$$

Rearranging gives:

$$\frac{\mu}{2} \|\mathbf{y} - \mathbf{x}\|^2 \geq \frac{\mu}{4} \|\mathbf{y} - \mathbf{z}\|^2 - \frac{\mu}{2} \|\mathbf{z} - \mathbf{x}\|^2.$$

Substituting this into the previous bound yields:

$$\langle \nabla h(\mathbf{x}), \mathbf{z} - \mathbf{y} \rangle \geq h(\mathbf{z}) - h(\mathbf{y}) + \frac{\mu}{4} \|\mathbf{y} - \mathbf{z}\|^2 - \left(\frac{L + \mu}{2} \right) \|\mathbf{z} - \mathbf{x}\|^2.$$

Since $\mu \leq L$, we have:

$$\langle \nabla h(\mathbf{x}), \mathbf{z} - \mathbf{y} \rangle \geq h(\mathbf{z}) - h(\mathbf{y}) + \frac{\mu}{4} \|\mathbf{y} - \mathbf{z}\|^2 - L \|\mathbf{z} - \mathbf{x}\|^2.$$

This completes the proof. □

In the next lemma we show in sampling with replacement and sampling without replacement, the expected sample mean $\bar{\mathbf{x}}_\pi$ equals the total mean $\bar{\mathbf{x}}$, while the variance associated to sample mean differs depending on whether sampling is with or without replacement.

Lemma 3. *Given a population of fixed vectors $\mathbf{x}_1, \mathbf{x}_2, \dots, \mathbf{x}_m$, we define the population mean and variance as follows:*

$$\bar{\mathbf{x}} := \frac{1}{m} \sum_{k=1}^m \mathbf{x}_k, \quad \nu^2 := \frac{1}{m} \sum_{k=1}^m \|\mathbf{x}_k - \bar{\mathbf{x}}\|^2.$$

Now, let s samples, denoted $\mathbf{x}_{\psi_1}, \mathbf{x}_{\psi_2}, \dots, \mathbf{x}_{\psi_s}$, be drawn from this population where $s \leq m$. Two common sampling approaches are: (i) Sampling with

Replacement, (ii) Sampling without Replacement. For both methods, we define the sample mean as $\bar{\mathbf{x}}_\psi := \frac{1}{s} \sum_{p=1}^s \mathbf{x}_{\psi_p}$. The expected value and variance of $\bar{\mathbf{x}}_\psi$ are given as follows:

Case I: For Sampling with Replacement:

$$\mathbb{E}[\bar{\mathbf{x}}_\psi] = \bar{\mathbf{x}}, \quad \mathbb{E}[\|\bar{\mathbf{x}}_\psi - \bar{\mathbf{x}}\|^2] = \frac{\nu^2}{s}, \quad (9)$$

Case II: For Sampling without Replacement:

$$\mathbb{E}[\bar{\mathbf{x}}_\psi] = \bar{\mathbf{x}}, \quad \mathbb{E}[\|\bar{\mathbf{x}}_\psi - \bar{\mathbf{x}}\|^2] = \frac{m-s}{s(m-1)}\nu^2. \quad (10)$$

Proof. Case I.

Let the population be $\{\mathbf{x}_1, \mathbf{x}_2, \dots, \mathbf{x}_m\}$ with population mean $\bar{\mathbf{x}}$. We draw s samples $\mathbf{x}_{\psi_1}, \mathbf{x}_{\psi_2}, \dots, \mathbf{x}_{\psi_s}$ with replacement. The sample mean is defined as: $\bar{\mathbf{x}}_\psi = \frac{1}{s} \sum_{j=1}^s \mathbf{x}_{\psi_j}$. The expected value of $\bar{\mathbf{x}}_\psi$ is:

$$\mathbb{E}[\bar{\mathbf{x}}_\psi] = \mathbb{E}\left[\frac{1}{s} \sum_{j=1}^s \mathbf{x}_{\psi_j}\right] = \frac{1}{s} \sum_{j=1}^s \mathbb{E}[\mathbf{x}_{\psi_j}].$$

Since each \mathbf{x}_{ψ_j} is drawn uniformly from the population:

$$\mathbb{E}[\mathbf{x}_{\psi_j}] = \bar{\mathbf{x}}, \quad \text{for all } j.$$

Therefore: $\mathbb{E}[\bar{\mathbf{x}}_\psi] = \frac{1}{s} \sum_{j=1}^s \bar{\mathbf{x}} = \bar{\mathbf{x}}$. We need to find:

$$\mathbb{E}[\|\bar{\mathbf{x}}_\psi - \bar{\mathbf{x}}\|^2] = \mathbb{E}\left[\left\|\frac{1}{s} \sum_{j=1}^s (\mathbf{x}_{\psi_j} - \bar{\mathbf{x}})\right\|^2\right].$$

Expanding the squared norm:

$$\begin{aligned} \mathbb{E}\left[\left\|\frac{1}{s} \sum_{j=1}^s (\mathbf{x}_{\psi_j} - \bar{\mathbf{x}})\right\|^2\right] &= \frac{1}{s^2} \mathbb{E}\left[\sum_{j=1}^s \|\mathbf{x}_{\psi_j} - \bar{\mathbf{x}}\|^2\right. \\ &\quad \left.+ 2 \sum_{1 \leq j < k \leq s} (\mathbf{x}_{\psi_j} - \bar{\mathbf{x}})^\top (\mathbf{x}_{\psi_k} - \bar{\mathbf{x}})\right]. \quad (11) \end{aligned}$$

For the first term (variance of individual samples):

$$\mathbb{E}[\|\mathbf{x}_{\psi_j} - \bar{\mathbf{x}}\|^2] = \nu^2, \quad \text{for each } j. \quad (12)$$

For the second term (cross terms), since the samples are drawn independently:

$$\mathbb{E}[(\mathbf{x}_{\psi_j} - \bar{\mathbf{x}})^\top (\mathbf{x}_{\psi_k} - \bar{\mathbf{x}})] = 0 \quad \text{for } j \neq k.$$

Thus:

$$\mathbb{E}[\|\bar{\mathbf{x}}_\psi - \bar{\mathbf{x}}\|^2] = \frac{1}{s^2} \sum_{j=1}^s \mathbb{E}[\|\mathbf{x}_{\psi_j} - \bar{\mathbf{x}}\|^2] = \frac{1}{s^2} \cdot s \cdot \nu^2 = \frac{\nu^2}{s}.$$

Case II: Sampling without Replacement

For sampling without replacement, we utilize the established result:

$$\mathbb{E}[\|\bar{\mathbf{x}}_\psi - \bar{\mathbf{x}}\|^2] = \frac{m-s}{s(m-1)} \nu^2.$$

This expression accounts for the fact that variance decreases when sampling without replacement due to the lack of independence among the selected samples.

To derive this result, consider the covariance between two distinct sampled units, \mathbf{x}_{ψ_j} and \mathbf{x}_{ψ_k} for $j \neq k$:

$$\begin{aligned} \text{Cov}(\mathbf{x}_{\psi_j}, \mathbf{x}_{\psi_k}) &= \mathbb{E}[\langle \mathbf{x}_{\psi_j} - \bar{\mathbf{x}}, \mathbf{x}_{\psi_k} - \bar{\mathbf{x}} \rangle] \\ &= \sum_{i=1}^m \sum_{k \neq i}^m \langle \mathbf{x}_i - \bar{\mathbf{x}}, \mathbf{x}_k - \bar{\mathbf{x}} \rangle \cdot \Pr(\mathbf{x}_{\psi_j} = \mathbf{x}_i, \mathbf{x}_{\psi_k} = \mathbf{x}_k). \end{aligned}$$

Since there are $m(m-1)$ possible pairs of $(\mathbf{x}_{\psi_j}, \mathbf{x}_{\psi_k})$, each occurring with equal probability, we find:

$$\Pr(\mathbf{x}_{\psi_j} = \mathbf{x}_i, \mathbf{x}_{\psi_k} = \mathbf{x}_k) = \frac{1}{m(m-1)}.$$

Consequently, the covariance can be expressed as:

$$\begin{aligned}
\text{Cov}(\mathbf{x}_{\psi_j}, \mathbf{x}_{\psi_k}) &= \frac{1}{m(m-1)} \sum_{i=1}^m \sum_{k \neq i}^m \langle \mathbf{x}_i - \bar{\mathbf{x}}, \mathbf{x}_k - \bar{\mathbf{x}} \rangle \\
&= \frac{1}{m(m-1)} \left\| \sum_{i=1}^m (\mathbf{x}_i - \bar{\mathbf{x}}) \right\|^2 \\
&\quad - \frac{1}{m(m-1)} \sum_{i=1}^m \|\mathbf{x}_i - \bar{\mathbf{x}}\|^2 = -\frac{\nu^2}{m-1}. \tag{13}
\end{aligned}$$

Using this covariance result, we can express the expected squared difference of the sample mean from the population mean as:

$$\mathbb{E} \|\bar{\mathbf{x}}_\psi - \bar{\mathbf{x}}\|^2 = \frac{\nu^2}{s} - \frac{s(s-1)}{s^2} \cdot \frac{\nu^2}{m-1} = \frac{(m-s)}{s(m-1)} \nu^2. \tag{14}$$

□

The next lemma provides a bound on the variance of sequentially sampled observations within the specified setup.

Lemma 4. *Consider a sequence of random variables $\{\xi_i\}_{i=1}^m$ and an associated sequence of random vectors $\{\mathbf{x}_i\}_{i=1}^m$, where each $\mathbf{x}_i \in \mathbb{R}^d$ depends on the history $\xi_1, \xi_2, \dots, \xi_i$. Assume that, for each i , the conditional expectation satisfies*

$$\mathbb{E}_{\xi_i}[\mathbf{x}_i \mid \xi_1, \dots, \xi_{i-1}] = \mathbf{e}_i.$$

This implies that $\{\mathbf{x}_i - \mathbf{e}_i\}_{i=1}^m$ is a martingale difference sequence with respect to the filtration generated by $\{\xi_i\}_{i=1}^m$. Additionally, suppose that the conditional variance of each $\mathbf{x}_i - \mathbf{e}_i$ is uniformly bounded, so that

$$\mathbb{E}_{\xi_i}[\|\mathbf{x}_i - \mathbf{e}_i\|^2 \mid \xi_1, \dots, \xi_{i-1}] \leq \delta^2,$$

for all $i = 1, \dots, m$, where $\delta > 0$ is a fixed constant. Now, using the “sampling without replacement” approach described in Lemma 3, let $p_{c,i}(k)$ be defined as follows:

$$p_{c,i}(k) = \begin{cases} I - 1, & \text{if } k \leq c - 1, \\ i - 1, & \text{if } k = c, \end{cases}$$

where I is a fixed integer. For $J \leq C$ and $C \geq 2$, the inequality below holds:

$$\sum_{c=1}^J \sum_{i=0}^{I-1} \mathbb{E} \left\| \sum_{k=1}^c \sum_{j=0}^{p_{c,i}(k)} (\mathbf{x}_{\psi_k} - \bar{\mathbf{x}}) \right\|^2 \leq \frac{1}{2} J^2 I^3 \nu^2. \quad (15)$$

Here, $\bar{\mathbf{x}}$ is the population mean, and ν^2 is the population variance, as defined in Lemma 3.

Proof. We start by expanding the left side of inequality (15):

$$\begin{aligned} & \mathbb{E} \left\| \sum_{k=1}^c \sum_{j=0}^{p_{c,i}(k)} (\mathbf{x}_{\psi_k} - \bar{\mathbf{x}}) \right\|^2 \\ &= \mathbb{E} \left\| I \sum_{k=1}^{c-1} (\mathbf{x}_{\psi_k} - \bar{\mathbf{x}}) + i(\mathbf{x}_{\psi_c} - \bar{\mathbf{x}}) \right\|^2 \\ &= I^2 \mathbb{E} \left\| \sum_{k=1}^{c-1} (\mathbf{x}_{\psi_k} - \bar{\mathbf{x}}) \right\|^2 + i^2 \mathbb{E} \|\mathbf{x}_{\psi_c} - \bar{\mathbf{x}}\|^2 \\ & \quad + 2Ii \mathbb{E} \left[\left\langle \sum_{k=1}^{c-1} (\mathbf{x}_{\psi_k} - \bar{\mathbf{x}}), (\mathbf{x}_{\psi_c} - \bar{\mathbf{x}}) \right\rangle \right]. \quad (16) \end{aligned}$$

To derive the closed quantity for the term $\mathbb{E} \left\| I \sum_{k=1}^{c-1} (\mathbf{x}_{\psi_k} - \bar{\mathbf{x}}) \right\|^2$, we can apply the results that we already computed in (11) and (14), which gives:

$$I^2 \mathbb{E} \left\| \sum_{k=1}^{c-1} (\mathbf{x}_{\psi_k} - \bar{\mathbf{x}}) \right\|^2 = \frac{(c-1)(C-(c-1))}{C-1} I^2 \nu^2,$$

this can be verified simply by replacing m with C and s with $c-1$ in (14). The term $i^2 \mathbb{E} \|\mathbf{x}_{\psi_c} - \bar{\mathbf{x}}\|^2 = i^2 \nu^2$, since it is the variance of an individual sample. Finally, we have

$$2Ii \mathbb{E} \left[\left\langle \sum_{k=1}^{c-1} (\mathbf{x}_{\psi_k} - \bar{\mathbf{x}}), (\mathbf{x}_{\psi_c} - \bar{\mathbf{x}}) \right\rangle \right] = -\frac{2(c-1)}{C-1} Ii \nu^2,$$

this can be simply verified by considering (13) since we have $c-1$ pairs and replacing m with c .

Summing the previous terms over c and i , we obtain:

$$\begin{aligned}
& \sum_{c=1}^J \sum_{i=0}^{I-1} \mathbb{E} \left[\left\| \sum_{k=1}^c \sum_{j=0}^{p_{c,i}(k)} (\mathbf{x}_{\psi_k} - \bar{\mathbf{x}}) \right\|^2 \right] \\
&= \frac{CI^3\nu^2}{C-1} \sum_{c=1}^J (c-1) - \frac{I^3\nu^2}{C-1} \sum_{c=1}^J (c-1)^2 \\
&\quad + J\nu^2 \sum_{i=0}^{I-1} i^2 - \frac{2I\nu^2}{C-1} \sum_{c=1}^J (c-1) \sum_{i=0}^{I-1} i. \quad (17)
\end{aligned}$$

Next, we apply the known summation formulas:

$$\sum_{i=1}^{I-1} i = \frac{(I-1)I}{2} \quad \text{and} \quad \sum_{i=1}^{I-1} i^2 = \frac{(I-1)I(2I-1)}{6}.$$

Substituting these results into the preceding equation simplifies it to:

$$\begin{aligned}
& \sum_{c=1}^J \sum_{i=0}^{I-1} \mathbb{E} \left[\left\| \sum_{k=1}^c \sum_{j=0}^{p_{c,i}(k)} (\mathbf{x}_{\psi_k} - \bar{\mathbf{x}}) \right\|^2 \right] \\
&= \nu^2 \left(\frac{1}{2} JI^2(JI-1) - \frac{1}{6} JI(I^2-1) \right. \\
&\quad \left. - \frac{1}{C-1} (J-1)JI^2 \left(\frac{1}{6}(2J-1)I - \frac{1}{2} \right) \right), \quad (18)
\end{aligned}$$

Finally, we can bound (18) by:

$$(\cdot) \leq \frac{1}{2} J^2 I^3 \nu^2,$$

which concludes the proof of this lemma (see appendix for derivation of the last equality in (18)). \square

Remark. In the context of AFL, the term inside the expectation (15) represents the accumulation of deviations between local model updates and the

global model over multiple clients and training iterations. Specifically, it quantifies the variance of these deviations, where each deviation measures the discrepancy between the local model update from a client and the central global model. The summation over clients and iterations reflects how these deviations accumulate as the training progresses, considering the asynchronous nature of the updates. The expectation operator is used to account for the inherent randomness in both the client participation (which may vary across rounds) and the local updates (often influenced by stochastic training methods such as stochastic gradient descent). By analyzing these accumulated deviations, the expression provides an upper bound on the total variance of the model updates, offering insight into the stability and convergence behavior of the FL process.

5. Convergence Analysis of AFL

In this section, we examine the convergence behavior of the proposed AFL algorithm in the context of a strongly convex setting. The local objectives are denoted as F_1, F_2, \dots, F_C .

5.1. Finding the recursion in Asynchronous Federated Learning

Suppose that Assumptions 1, 2, and 3b are satisfied, and that each local objective function is μ -strongly convex. We also introduce the following additional assumptions specific to AFL:

Assumption 3e. *The global model update is asynchronous, meaning updates from clients are applied without waiting for all clients to finish.*

Assumption 3f. *Each client c has an update delay τ_c , representing the difference between the time when client c computes its gradient and when that gradient is applied to the global model.*

Assumption 3g. *Gradients are based on possibly stale versions of the global model.*

We start by deriving a closed formula for the recursion updates for the clients in the AFL.

Lemma 5. *If the learning rate satisfies $\lambda \leq \frac{1}{6LJI}$, then we have:*

$$\begin{aligned}
\mathbb{E} [\|\mathbf{x}^{(j+1)} - \mathbf{x}^*\|^2] &\leq \left(1 - \frac{\mu J I \lambda}{2}\right) \mathbb{E} [\|\mathbf{x}^{(j)} - \mathbf{x}^*\|^2] \\
&\quad + 4JI\lambda^2\delta^2 + 4J^2I^2\lambda^2 \frac{C-J}{J(C-1)} \nu_*^2 \\
&\quad - \frac{2}{3}JI\lambda \mathbb{E} [D_F(\mathbf{x}^{(j)}, \mathbf{x}^*)] \\
&\quad + \frac{8}{3}L\lambda \sum_{c=1}^J \sum_{i=0}^{I-1} \mathbb{E} [\|\mathbf{x}_{c,i}^{(j)} - \mathbf{x}^{(j-\tau_c)}\|^2] \tag{19}
\end{aligned}$$

Proof. Based on the Algorithm 1, the general update formula in AFL when we complete a full training round with J randomly selected clients are given by:

$$\Delta \mathbf{x} = \mathbf{x}^{(j+1)} - \mathbf{x}^{(j)} = -\lambda \sum_{c=1}^J \sum_{i=0}^{I-1} \mathbf{q}_{\psi_c,i}^{(j)}, \tag{20}$$

and

$$\mathbb{E} [\Delta \mathbf{x}] = -\lambda \sum_{c=1}^J \sum_{i=0}^{I-1} \mathbb{E} \left[\nabla F_{\psi_c}(\mathbf{x}_{c,i}^{(j-\nu)}) \right], \tag{21}$$

where $\mathbf{q}_{\psi_c,i}^{(j)} = \nabla f_{\psi_c}(\mathbf{x}_{c,i}^{(j)}; \xi)$ represents the stochastic gradient of F_{ψ_c} with respect to $\mathbf{x}_{c,i}^{(j)}$. To simplify notation, we address a single training round and temporarily omit superscript j . We refer to $\mathbf{x}_{c,i}^{(j)}$ as $\mathbf{x}_{c,i}$ and set $\mathbf{x}_{1,0}^{(j)} = \mathbf{x}$. Unless specified otherwise, all expectations are conditioned on $\mathbf{x}^{(j)}$. Starting from the equation (19):

$$\mathbb{E} \|\mathbf{x} + \Delta \mathbf{x} - \mathbf{x}^*\|^2 = \|\mathbf{x} - \mathbf{x}^*\|^2 + 2\mathbb{E} [\langle \mathbf{x} - \mathbf{x}^*, \Delta \mathbf{x} \rangle] + \mathbb{E} \|\Delta \mathbf{x}\|^2, \tag{22}$$

we substitute the overall updates $\Delta \mathbf{x}$ and proceed using the results of Lemma 2

with $\mathbf{x} = \mathbf{x}_{c,i}$, $\mathbf{y} = \mathbf{x}^*$, $\mathbf{z} = \mathbf{x}$ and $h = F_{\psi_c}$ for the first inequality (see (8)):

$$\begin{aligned}
& 2\mathbb{E} [\langle \mathbf{x} - \mathbf{x}^*, \Delta \mathbf{x} \rangle] \\
&= -2\lambda \sum_{c=1}^J \sum_{i=0}^{I-1} \mathbb{E} \left[\left\langle \nabla F_{\psi_c}(\mathbf{x}_{c,i}^{(j-\nu)}), \mathbf{x} - \mathbf{x}^* \right\rangle \right] \\
&\leq -2\lambda \sum_{c=1}^J \sum_{i=0}^{I-1} \mathbb{E} \left[F_{\psi_c}(\mathbf{x}) - F_{\psi_c}(\mathbf{x}^*) \right. \\
&\quad \left. + \frac{\mu}{4} \|\mathbf{x} - \mathbf{x}^*\|^2 - L \|\mathbf{x}_{c,i} - \mathbf{x}\|^2 \right] \\
&\leq -2JI\lambda D_F(\mathbf{x}, \mathbf{x}^*) - \frac{1}{2}\mu JI\lambda \|\mathbf{x} - \mathbf{x}^*\|^2 \\
&\quad + 2L\lambda \sum_{c=1}^J \sum_{i=0}^{I-1} \mathbb{E} \|\mathbf{x}_{c,i} - \mathbf{x}\|^2.
\end{aligned}$$

For the term $\mathbb{E} \|\Delta \mathbf{x}\|^2$, we consider the asynchronous updates:

$$\begin{aligned}
\mathbb{E} \|\Delta \mathbf{x}\|^2 &\leq 4\lambda^2 \mathbb{E} \left\| \sum_{c=1}^J \sum_{i=0}^{I-1} \left(\mathbf{q}_{\psi_c,i} - \nabla F_{\psi_c}(\mathbf{x}_{c,i}^{(j-\tau_c)}) \right) \right\|^2 \\
&\quad + 4\lambda^2 \mathbb{E} \left\| \sum_{c=1}^J \sum_{i=0}^{I-1} \left(\nabla F_{\psi_c}(\mathbf{x}_{c,i}^{(j-\tau_c)}) - \nabla F_{\psi_c}(\mathbf{x}) \right) \right\|^2 \\
&\quad + 4\lambda^2 \mathbb{E} \left\| \sum_{c=1}^J \sum_{i=0}^{I-1} \left(\nabla F_{\psi_c}(\mathbf{x}) - \nabla F_{\psi_c}(\mathbf{x}^*) \right) \right\|^2 \\
&\quad + 4\lambda^2 \mathbb{E} \left\| \sum_{c=1}^J \sum_{i=0}^{I-1} \nabla F_{\psi_c}(\mathbf{x}^*) \right\|^2. \tag{23}
\end{aligned}$$

We will now bound the terms on the right-hand side of Inequality (23) similarly to before; for the first term from the results of Lemma 1 and assumption 2 we have:

$$4\lambda^2 \sum_{c=1}^C \sum_{i=0}^{I-1} \mathbb{E} \left\| \mathbf{q}_{\psi_c,i} - \nabla F_{\psi_c}(\mathbf{x}_{c,i}^{(j-\tau_c)}) \right\|^2 \leq 4\lambda^2 CI\delta^2.$$

For the second term from assumption 1 we have:

$$\begin{aligned}
4\lambda^2 \mathbb{E} \left\| \sum_{c=1}^J \sum_{i=0}^{I-1} \left(\nabla F_{\psi_c}(\mathbf{x}_{c,i}^{(j-\tau_c)}) - \nabla F_{\psi_c}(\mathbf{x}) \right) \right\|^2 \\
\leq 4\lambda^2 JI \sum_{c=1}^J \sum_{i=0}^{I-1} \mathbb{E} \left\| \nabla F_{\psi_c}(\mathbf{x}_{c,i}^{(j-\tau_c)}) - \nabla F_{\psi_c}(\mathbf{x}) \right\|^2 \\
\leq 4L^2 \lambda^2 JI \sum_{c=1}^J \sum_{i=0}^{I-1} \mathbb{E} \|\mathbf{x}_{c,i} - \mathbf{x}\|^2.
\end{aligned}$$

For the third term in (23) from assumption 1 and the property of convex functions (inequality 5):

$$\begin{aligned}
4\lambda^2 \mathbb{E} \left\| \sum_{c=1}^J \sum_{i=0}^{I-1} \left(\nabla F_{\psi_c}(\mathbf{x}) - \nabla F_{\psi_c}(\mathbf{x}^*) \right) \right\|^2 \\
\leq 4\lambda^2 JI \sum_{c=1}^J \sum_{i=0}^{I-1} \mathbb{E} \|\nabla F_{\psi_c}(\mathbf{x}) - \nabla F_{\psi_c}(\mathbf{x}^*)\|^2 \\
\leq 8L\lambda^2 JI \sum_{c=1}^J \sum_{i=0}^{I-1} \mathbb{E} [D_{F_{\psi_c}}(\mathbf{x}, \mathbf{x}^*)] \\
\leq 8L\lambda^2 J^2 I^2 D_F(\mathbf{x}, \mathbf{x}^*).
\end{aligned}$$

For the fourth term from results of Lemma 3:

$$4\lambda^2 \mathbb{E} \left\| \sum_{c=1}^J \sum_{i=0}^{I-1} \nabla F_{\psi_c}(\mathbf{x}^*) \right\|^2 \leq 4\lambda^2 J^2 I^2 \frac{C-J}{J(C-1)} \nu_*^2.$$

We consider the data sample $\xi_{c,i}$, the stochastic gradient $\mathbf{e}_{\psi_c,i}$, and the gradient $\nabla F_{\psi_c}(\xi_{c,i})$ as ξ_k , \mathbf{x}_k , and \mathbf{e}_k in Lemma 1, and then apply the consequences of Lemma 1 to the first term on the right-hand side of inequality (23).

With the bounds for the terms in inequality (23), we get

$$\begin{aligned}
\mathbb{E} \|\Delta \mathbf{x}\|^2 &\leq 4\lambda^2 JI \delta^2 + 4J^2 I^2 \lambda^2 \frac{J-I}{J(J-1)} \nu_*^2 \\
&\quad + 8L\lambda^2 J^2 I^2 D_F(\mathbf{x}, \mathbf{x}^*) \\
&\quad + 4L^2 \lambda^2 JI \sum_{c=1}^J \sum_{i=0}^{I-1} \mathbb{E} [\|\mathbf{x}_{c,i} - \mathbf{x}\|^2].
\end{aligned}$$

Putting back the bounds of $2\mathbb{E}[\langle \mathbf{x} - \mathbf{x}^*, \Delta \mathbf{x} \rangle]$ and $\mathbb{E} \|\Delta \mathbf{x}\|^2$, and using $\lambda \leq \frac{1}{6LCI}$, yields

$$\begin{aligned} \mathbb{E} \|\mathbf{x} + \Delta \mathbf{x} - \mathbf{x}^*\|^2 &\leq \left(1 - \frac{\mu J I \lambda}{2}\right) \|\mathbf{x} - \mathbf{x}^*\|^2 \\ &\quad + 4JI\lambda^2\delta^2 + 4J^2I^2\lambda^2 \frac{C - J}{J(C - 1)} \nu_*^2 \\ &\quad - \frac{2}{3}CI\lambda D_F(\mathbf{x}, \mathbf{x}^*) \\ &\quad + \frac{8}{3}L\lambda \sum_{c=1}^J \sum_{i=0}^{I-1} \mathbb{E} [\|\mathbf{x}_{c,i} - \mathbf{x}\|^2]. \end{aligned} \quad (24)$$

If we take unconditional expectation and reinstating the superscripts, then it completes the proof. We can substitute them back into the recursion relation and simplify to obtain the desired inequality for AFL. \square

Building on the concept of “client drift” in PFL Karimireddy et al. [8], we define the client drift in AFL with Assumption 3b as follows (see also the last term in (24)):

$$E_j := \sum_{c=1}^J \sum_{i=0}^{I-1} \mathbb{E} \left[\left\| \mathbf{x}_{c,i}^{(j)} - \mathbf{x}^{(j)} \right\|^2 \right] \quad (25)$$

where E_j quantifies the drift of client parameters from the global model across all clients and local updates.

The following lemma provides a bound on the client drifts from the global model.

Lemma 6. *Suppose that Assumptions 1, 2, and 3b are satisfied, and that each local objective function is μ -strongly convex. Additionally, if the step size η is chosen such that $\eta \leq \frac{1}{6LCI}$, then the drift in the client updates is bounded by the following inequality:*

$$E_j \leq \frac{9}{4}J^2I^2\lambda^2\delta^2 + \frac{9}{4}J^2I^3\lambda^2\nu_*^2 + 3LJ^3I^3\lambda^2\mathbb{E} [D_F(\mathbf{x}^{(j)}, \mathbf{x}^*)]. \quad (26)$$

Proof. In the asynchronous setting, client updates do not occur simultaneously, which introduces a time delay into the analysis. Let $\mathbf{x}^{(j)}$ denote the

global model at round j and $\mathbf{x}_{c,i}^{(j)}$ the update from client c at step i within round j . Due to asynchronicity, $\mathbf{x}_{c,i}^{(j)}$ may be computed based on a stale global model $\mathbf{x}^{(j-\tau_{c,i})}$, where $\tau_{c,i} \geq 0$ represents the staleness (or delay) of the model used by client c at step i .

Following Algorithm 1, the update rule for AFL from $\mathbf{x}^{(j-\tau_{c,i})}$ to $\mathbf{x}_{c,i}^{(j)}$ can be written as

$$\mathbf{x}_{c,i}^{(j)} - \mathbf{x}^{(j-\tau_{c,i})} = -\lambda \sum_{k=1}^c \sum_{l=0}^{p_{c,i}(k)} \mathbf{q}_{\psi_k,l}^{(j)}$$

with $p_{c,i}(k) := \begin{cases} I-1, & k \leq c-1, \\ i-1, & k = c. \end{cases}$

Similar to Lemma 5 for the sake of simplicity, we consider a single training round, and hence we suppress in our notation the superscripts j temporarily, assuming all expectations are conditioned on $\mathbf{x}^{(j)}$ unless otherwise stated.

To bound $\mathbb{E} \|\mathbf{x}_{c,i} - \mathbf{x}\|^2$ in an asynchronous setting, we use the fact that $\mathbf{x}_{c,i}$ is computed based on a potentially stale model, introducing additional variance from the delay. This gives:

$$\begin{aligned} & \mathbb{E} \|\mathbf{x}_{c,i} - \mathbf{x}\|^2 \\ & \leq 4\lambda^2 \mathbb{E} \left\| \sum_{k=1}^c \sum_{l=0}^{p_{c,i}(k)} (\mathbf{q}_{\psi_k,l} - \nabla F_{\psi_k}(\mathbf{x}_{k,l})) \right\|^2 \\ & \quad + 4\lambda^2 \mathbb{E} \left\| \sum_{k=1}^c \sum_{l=0}^{p_{c,i}(k)} (\nabla F_{\psi_k}(\mathbf{x}_{k,l}) - \nabla F_{\psi_k}(\mathbf{x})) \right\|^2 \\ & \quad + 4\lambda^2 \mathbb{E} \left\| \sum_{k=1}^c \sum_{l=0}^{p_{c,i}(k)} (\nabla F_{\psi_k}(\mathbf{x}) - \nabla F_{\psi_k}(\mathbf{x}^*)) \right\|^2 \\ & \quad + 4\lambda^2 \underbrace{\mathbb{E} \left\| \sum_{k=1}^c \sum_{l=0}^{p_{c,i}(k)} \nabla F_{\psi_k}(\mathbf{x}^*) \right\|^2}_{T_{c,i}}. \end{aligned} \tag{27}$$

Next, we will find bounds for each term in the right-hand side of (27). We apply Lemma 1 and Jensen's inequality as before, but now with adjustments for the staleness $\tau_{c,i}$, in this regard from Lemma 1, Assumption 2

$$\begin{aligned}
4\lambda^2 \mathbb{E} \left\| \sum_{i=1}^m \sum_{j=0}^{p_{m,k}(i)} (\mathbf{g}_{\psi_i,j} - \nabla F_{\psi_i}(\mathbf{x}_{i,j})) \right\|^2 \\
\leq 4\lambda^2 \sum_{i=1}^m \sum_{j=0}^{p_{m,k}(i)} \mathbb{E} \|\mathbf{g}_{\psi_i,j} - \nabla F_{\psi_i}(\mathbf{x}_{i,j})\|^2 \\
\leq 4\lambda^2 \mathcal{B}_{m,k} \delta^2, \quad (28)
\end{aligned}$$

from Assumption 2 we have

$$\begin{aligned}
4\lambda^2 \mathbb{E} \left\| \sum_{i=1}^m \sum_{j=0}^{p_{m,k}(i)} (\nabla F_{\psi_i}(\mathbf{x}_{i,j}) - \nabla F_{\psi_i}(\mathbf{x})) \right\|^2 \\
\leq 4\lambda^2 \mathcal{B}_{m,k} \sum_{i=1}^m \sum_{j=0}^{p_{m,k}(i)} \mathbb{E} \|\nabla F_{\psi_i}(\mathbf{x}_{i,j}) - \nabla F_{\psi_i}(\mathbf{x})\|^2 \\
\leq 4L^2 \lambda^2 \mathcal{B}_{m,k} \sum_{i=1}^m \sum_{j=0}^{p_{m,k}(i)} \mathbb{E} \|\mathbf{x}_{i,j} - \mathbf{x}\|, \quad (29)
\end{aligned}$$

from Assumption 2 and convex property (5) we have

$$\begin{aligned}
4\lambda^2 \mathbb{E} \left\| \sum_{i=1}^m \sum_{j=0}^{p_{m,k}(i)} (\nabla F_{\psi_i}(\mathbf{x}) - \nabla F_{\psi_i}(\mathbf{x}^*)) \right\|^2 \\
\leq 4\lambda^2 \mathcal{B}_{m,k} \sum_{i=1}^m \sum_{j=0}^{p_{m,k}(i)} \mathbb{E} \|\nabla F_{\psi_i}(\mathbf{x}) - \nabla F_{\psi_i}(\mathbf{x}^*)\|^2 \\
\leq 8L\lambda^2 \mathcal{B}_{m,k} \sum_{i=1}^m \sum_{j=0}^{p_{m,k}(i)} \mathbb{E} \left[D_{F_{\psi_i}}(\mathbf{x}, \mathbf{x}^*) \right], \quad (30)
\end{aligned}$$

where $\mathcal{B}_{m,k} = \sum_{i=1}^m \sum_{j=0}^{p_{m,k}(i)} 1 = (m-1)I + k$. Now, we incorporate these

bounds into the expression for E_j , yielding:

$$\begin{aligned}
E_j &\leq 4\lambda^2\delta^2 \sum_{m=1}^J \sum_{i=0}^{I-1} \mathcal{B}_{m,i} \\
&\quad + 4L^2\lambda^2 \sum_{m=1}^J \sum_{i=0}^{I-1} \mathcal{B}_{m,i} \sum_{k=1}^m \sum_{j=0}^{p_{m,i}(k)} \mathbb{E} \|\mathbf{x}_{k,j} - \mathbf{x}\|^2 \\
&\quad + 8L\lambda^2 \sum_{m=1}^J \sum_{i=0}^{I-1} \mathcal{B}_{m,i}^2 D_F(\mathbf{x}, \mathbf{x}^*) \\
&\quad + 4\lambda^2 \sum_{m=1}^J \sum_{i=0}^{I-1} T_{m,i}.
\end{aligned}$$

For the fourth term from the results of Lemma 4 by setting $\mathbf{x}_{\psi_i} = \nabla F_{\psi_i}(\mathbf{x}^*)$, $\bar{x} = \nabla F(\mathbf{x}^*) = 0$, and knowing that $\sum_{m=1}^J \sum_{i=0}^{I-1} \mathcal{B}_{m,i} \leq \frac{1}{2}J^2I^2$ and $\sum_{m=1}^J \sum_{i=0}^{I-1} \mathcal{B}_{m,i}^2 \leq \frac{1}{3}J^3I^3$,

$$4\lambda^2 \mathbb{E} \left\| \sum_{k=1}^c \sum_{j=0}^{p_{c,i}(k)} \nabla F_{\psi_k}(\mathbf{x}^*) \right\|^2 \leq 4\lambda^2 \times \frac{1}{2}J^2I^3\nu_*^2, \quad (31)$$

then we have:

$$\begin{aligned}
E_j &\leq 2J^2I^2\lambda^2\delta^2 + 2L^2J^2I^2\lambda^2E_j \\
&\quad + \frac{8}{3}LJ^3I^3\lambda^2D_F(\mathbf{x}, \mathbf{x}^*) + 2J^2I^3\lambda^2\nu_*^2.
\end{aligned}$$

Finally, after rearranging and applying the condition $\lambda \leq \frac{1}{6LJI}$, we obtain:

$$E_j \leq \frac{9}{4}J^2I^2\lambda^2\delta^2 + \frac{9}{4}J^2I^3\lambda^2\nu_*^2 + 3LJ^3I^3\lambda^2D_F(\mathbf{x}, \mathbf{x}^*).$$

This completes the proof. \square

Inspired by Karimireddy et al. [8], in the next lemma we give an upper bound on the weighted sum of gradients for a learning process with a time-varying learning rate, incorporating the effects of asynchronous delays, which serves as a key step in establishing the convergence properties of AFL.

Lemma 7. We consider two non-negative sequences $\{d_t\}_{t \geq 0}$, $\{g_t\}_{t \geq 0}$, which satisfy the relation

$$d_{t+1} \leq (1 - a\gamma)d_t - b\gamma g_t + l\gamma^2, \quad \forall t > 0 \quad (32)$$

where parameters $z > 0$, v , $l \geq 0$ and the learning rate γ_t defined as

$$\gamma_t = \frac{\gamma_0}{\sqrt{t+1} \cdot (1 + \alpha \cdot \tau_t)}, \quad (33)$$

where γ_0 is a constant, $1 \geq \alpha \geq 0$ is a constant controlling asynchronous delays, and τ_t represents the time-varying delays. In this regard, there is a learning rate γ_t as defined in (33), and weights $\pi_t = (1 - z\gamma_t)^{(t+1)}$ with $\Pi_T := \sum_{t=0}^T \pi_t$, such that the following bound holds:

$$\Psi_T := \frac{1}{\Pi_T} \sum_{t=0}^T g_t \pi_t \leq \frac{(z\gamma_0)^2 \pi_0 d_0}{2v\gamma_0} + \frac{z\gamma_0^2 l}{2}.$$

Proof. Starting from the original inequality:

$$d_{t+1} \leq (1 - z\gamma_t)d_t - v\gamma_t g_t + l\gamma_t^2,$$

where $\gamma_t = \frac{\gamma_0}{\sqrt{t+1} \cdot (1 + \alpha \cdot \tau_t)}$, doing some manipulation and multiplying both sides by π_t :

$$v g_t \pi_t \leq \frac{\pi_t (1 - z\gamma_t) d_t}{\gamma_t} - \frac{\pi_t d_{t+1}}{\gamma_t} + l \gamma_t \pi_t.$$

Substituting $\gamma_t = \frac{\gamma_0}{\sqrt{t+1} \cdot (1 + \alpha \cdot \tau_t)}$, we rewrite this as:

$$\begin{aligned} v g_t \pi_t \leq & \frac{\pi_t \left(1 - z \cdot \frac{\gamma_0}{\sqrt{t+1} \cdot (1 + \alpha \cdot \tau_t)} \right) d_t}{\frac{\gamma_0}{\sqrt{t+1} \cdot (1 + \alpha \cdot \tau_t)}} \\ & - \frac{\pi_t d_{t+1}}{\frac{\gamma_0}{\sqrt{t+1} \cdot (1 + \alpha \cdot \tau_t)}} + l \frac{\gamma_0}{\sqrt{t+1} \cdot (1 + \alpha \cdot \tau_t)} \pi_t. \end{aligned} \quad (34)$$

Simplifying each term, we obtain:

$$v g_t \pi_t \leq \frac{\pi_{t-1} d_t}{\gamma_t} - \frac{\pi_t d_{t+1}}{\gamma_t} + l \gamma_t \pi_t.$$

Next, summing both sides from $t = 0$ to $t = T$ results in a telescoping sum:

$$v \sum_{t=0}^T g_t \pi_t \leq \sum_{t=0}^T \left(\frac{\pi_{t-1} d_t}{\gamma_t} - \frac{\pi_t d_{t+1}}{\gamma_t} \right) + l \sum_{t=0}^T \gamma_t \pi_t.$$

Dividing both sides by $\Pi_T := \sum_{t=0}^T \pi_t$, we get:

$$\Psi_T := \frac{1}{\Pi_T} \sum_{t=0}^T g_t \pi_t \leq \frac{1}{v \Pi_T} \left(\frac{\pi_0 (1 - z \gamma_0) d_0}{\gamma_0} - \frac{\pi_T d_{T+1}}{\gamma_T} \right) + \frac{1}{\Pi_T} \sum_{t=0}^T l \gamma_t w_t. \quad (35)$$

To find an upper bound for $\Pi_T = \sum_{t=0}^T \pi_t$ as $T \rightarrow \infty$, we will analyze the weights more carefully using the given learning rate and examine the behavior of the sum. Given:

$$\gamma_t = \frac{\gamma_0}{\sqrt{t+1} \cdot (1 + \alpha \cdot \tau_t)},$$

where γ_0 is a constant, $0 \leq \alpha \leq 1$ controls asynchronous delays, and τ_t represents time-varying delays. The weights π_t are defined as:

$$\pi_t = (1 - z \gamma_t)^{t+1}.$$

For small γ_t , we approximate $(1 - z \gamma_t) \approx e^{-z \gamma_t}$, so:

$$\pi_t \approx e^{-z \gamma_t (t+1)}.$$

Substituting the expression for γ_t , we get:

$$\pi_t \approx e^{-\frac{z \gamma_0 (t+1)}{\sqrt{t+1} \cdot (1 + \alpha \cdot \tau_t)}}.$$

Now, we approximate Π_T by summing (or integrating) over this expression. For large t , $\gamma_t \approx \frac{\gamma_0}{\sqrt{t}}$, so $\pi_t \approx e^{-z \gamma_0 \sqrt{t}}$. Thus:

$$\Pi_T \approx \sum_{t=0}^T e^{-z \gamma_0 \sqrt{t}}.$$

To approximate this sum, we can use the integral test, which suggests:

$$\Pi_T \approx \int_0^T e^{-z\gamma_0\sqrt{t}} dt.$$

Let $u = \sqrt{t}$, so $t = u^2$ and $dt = 2u du$. Then:

$$\Pi_T \approx \int_0^{\sqrt{T}} e^{-z\gamma_0 u} \cdot 2u du = 2 \int_0^{\sqrt{T}} u e^{-z\gamma_0 u} du.$$

This integral can be computed by parts. Letting $v = u$ and $dw = e^{-z\gamma_0 u} du$, we find:

$$\begin{aligned} \int u e^{-z\gamma_0 u} du &= -\frac{u}{z\gamma_0} e^{-z\gamma_0 u} + \frac{1}{z\gamma_0} \int e^{-z\gamma_0 u} du, \\ &= -\frac{u}{z\gamma_0} e^{-z\gamma_0 u} - \frac{1}{(z\gamma_0)^2} e^{-z\gamma_0 u}. \end{aligned}$$

Evaluating from 0 to \sqrt{T} :

$$\Pi_T \approx 2 \left(-\frac{\sqrt{T}}{z\gamma_0} e^{-z\gamma_0\sqrt{T}} - \frac{1}{(z\gamma_0)^2} e^{-z\gamma_0\sqrt{T}} + \frac{1}{(z\gamma_0)^2} \right).$$

As $T \rightarrow \infty$, the exponential terms $e^{-z\gamma_0\sqrt{T}}$ decay to zero, so the dominant term is:

$$\Pi_T \approx \frac{2}{(z\gamma_0)^2}. \quad (36)$$

To find a bound for the sum $\sum_{t=0}^T \gamma_t \pi_t$, we need to understand the asymptotic behavior of both γ_t and π_t .

- $\gamma_t = \frac{\gamma_0}{\sqrt{t+1} \cdot (1+\alpha \cdot \tau_t)}$ decreases as t increases. For large t , we can approximate $\gamma_t \approx \frac{\gamma_0}{\sqrt{t+1}}$, assuming $\alpha \cdot \tau_t$ remains relatively small (which we can do for simplicity).
- $\pi_t = (1 - z\gamma_t)^{(t+1)}$ behaves similarly to an exponential function. For large t , we can approximate $\pi_t \approx e^{-z\gamma_t(t+1)}$. Using the approximation for γ_t , we get:

$$\pi_t \approx e^{-z \cdot \frac{\gamma_0}{\sqrt{t+1}}(t+1)},$$

This suggests that π_t decays exponentially with increasing t . Given that $\gamma_t \approx \frac{\gamma_0}{\sqrt{t+1}}$ and $\pi_t \approx e^{-z \cdot \frac{\gamma_0}{\sqrt{t+1}}(t+1)}$, we expect the sum to behave asymptotically as:

$$\sum_{t=0}^T \gamma_t \pi_t \leq \sum_{t=0}^T \frac{\gamma_0}{\sqrt{t+1}} \cdot e^{-z \cdot \frac{\gamma_0}{\sqrt{t+1}}(t+1)}.$$

This sum is dominated by the initial terms, as the exponential decay will cause the later terms to contribute much less. For large T , we can approximate the sum by taking the first few terms, and we expect the sum to grow asymptotically like:

$$\sum_{t=0}^T \gamma_t \pi_t \approx \mathcal{O}\left(\frac{\gamma_0}{z}\right), \quad (37)$$

where z is the decay factor. Now that we have the bound for $\sum_{t=0}^T \gamma_t \pi_t \approx \frac{\gamma_0}{z}$, we can substitute this into the expression for Ψ_T . For large T as mentioned earlier, the term $\frac{1}{\Pi_T}$ becomes:

$$\frac{1}{\Pi_T} \approx \frac{(z\gamma_0)^2}{2}.$$

Substitute this into equation (35):

$$\Psi_T \leq \frac{(z\gamma_0)^2}{2} \cdot \left[\frac{1}{v} \left(\frac{\pi_0(1-z\gamma_0)d_0}{\gamma_0} - \frac{\pi_T d_{T+1}}{\gamma_T} \right) + \frac{\gamma_0}{z} \cdot l \right].$$

The final simplified expression for Ψ_T is:

$$\Psi_T \leq \frac{(z\gamma_0)^2}{2v} \left(\frac{\pi_0(1-z\gamma_0)d_0}{\gamma_0} - \frac{\pi_T r_{T+1}}{\gamma_T} \right) + \frac{(z\gamma_0)^2 l}{2z}.$$

This is the final simplified form of Ψ_T , incorporating the bounds for the sums as $T \rightarrow \infty$. We can simplify further the above relation by neglecting the terms $-\frac{\pi_T d_{T+1}}{\gamma_T}$ and $-z\gamma_0$, hence we end up with $\frac{(z\gamma_0)^2 \pi_0 d_0}{2v\gamma_0}$. To analyze the convergence rate of Ψ_T , let's examine the inequality established in Lemma 7:

$$\Psi_T := \frac{1}{\prod_T} \sum_{t=0}^T g_t \pi_t \leq \frac{(z\gamma_0)^2 \pi_0 d_0}{2v\gamma_0} + \frac{z\gamma_0^2 l}{2}.$$

Here, we can see that Ψ_T is bounded by terms involving γ_0 , z , v , l , and d_0 . □

Theorem 1. *Assume the objective functions of local clients are L -smooth (see Assumption 1) and strongly convex. In the AFL algorithm (see Algorithm 1), having Assumptions 2, 3b, with the learning rate $\tilde{\lambda} := \lambda CI$, weights $\{\pi_j\}_{j \geq 0}$, and weighted average of the global parameters $\bar{\mathbf{x}}^{(J)} := \frac{\sum_{j=0}^J \pi_j \mathbf{x}^{(j)}}{\sum_{j=0}^J \pi_j}$, there is a $\tilde{\lambda} \leq \frac{1}{6L}$ and $\pi_j = (1 - \frac{\mu\tilde{\lambda}}{2})^{(j+1)}$ that satisfies:*

$$\begin{aligned} \mathbb{E} [\mathcal{F}(\bar{\mathbf{x}}^{(J)}) - \mathcal{F}(\mathbf{x}^*)] &\leq \frac{9}{2} \mu \|\mathbf{x}^{(0)} - \mathbf{x}^*\|^2 \exp\left(-\frac{\mu\tilde{\lambda}J}{2}\right) + \frac{12\tilde{\lambda}\delta^2}{CI} + \frac{18L\tilde{\lambda}^2\delta^2}{CI} \\ &\quad + \frac{18L\tilde{\lambda}^2\nu_*^2}{C}. \end{aligned}$$

Proof. Applying the results of Lemmas 5 and 6, along with the condition $\lambda \leq \frac{1}{6LJK}$, we derive:

$$\begin{aligned} \mathbb{E} [\|\mathbf{x}^{(j+1)} - \mathbf{x}^*\|^2] &\leq \underbrace{\left(1 - \frac{\mu J I \lambda}{2}\right) \mathbb{E} [\|\mathbf{x}^{(j)} - \mathbf{x}^*\|^2]}_{\text{Contraction term}} - \underbrace{\frac{1}{3} J I \lambda \mathbb{E} [D_F(\mathbf{x}^{(j)}, \mathbf{x}^*)]}_{\text{Regularization term}} \\ &\quad + \underbrace{\frac{4 J I \lambda^2 \delta^2}{J(C-1)}}_{\text{Noise term 1}} + \underbrace{4 J^2 I^2 \lambda^2 \nu_*^2}_{\text{Noise term 2}} + \underbrace{\frac{6 L J^2 I^2 \lambda^3 \delta^2}{J(C-1)}}_{\text{Higher-order noise 1}} + \underbrace{\frac{6 L J^2 I^3 \lambda^3 \nu_*^2}{J(C-1)}}_{\text{Higher-order noise 2}}. \end{aligned}$$

Letting $\tilde{\lambda} = J I \lambda$, the bound simplifies:

$$\begin{aligned} \mathbb{E} [\|\mathbf{x}^{(j+1)} - \mathbf{x}^*\|^2] &\leq \left(1 - \frac{\mu\tilde{\lambda}}{2}\right) \mathbb{E} [\|\mathbf{x}^{(j)} - \mathbf{x}^*\|^2] - \frac{\tilde{\lambda}}{3} \mathbb{E} [D_F(\mathbf{x}^{(j)}, \mathbf{x}^*)] \\ &\quad + \frac{4\tilde{\lambda}^2\delta^2}{CI} + \frac{4\tilde{\lambda}^2(C-J)\nu_*^2}{S(C-1)} + \frac{6L\tilde{\lambda}^3\delta^2}{CI} + \frac{6L\tilde{\lambda}^3\nu_*^2}{J}. \end{aligned}$$

Now, leveraging Lemma 7, with: $t = j$, $T = \mathcal{J}$, $\gamma = \tilde{\lambda}$, $d_t = \mathbb{E} [\|\mathbf{x}^{(j)} - \mathbf{x}^*\|^2]$,
 $a = \frac{\mu}{2}$, $b = \frac{1}{3}$, $g_t = \mathbb{E} [D_F(\mathbf{x}^{(j)}, \mathbf{x}^*)]$, $w_t = (1 - \frac{\mu\tilde{\lambda}}{2})^{-(j+1)}$, $l_1 = \frac{4\delta^2}{CI} + \frac{4(C-J)\nu_*^2}{J(C-1)}$,
 $l_2 = \frac{6L\delta^2}{CI} + \frac{6L\nu_*^2}{J}$,
we reach to the performance bound:

$$\begin{aligned} \mathbb{E} [F(\bar{\mathbf{x}}^{(J)}) - F(\mathbf{x}^*)] &\leq \underbrace{\frac{9}{2}\mu\|\mathbf{x}^{(0)} - \mathbf{x}^*\|^2 \exp\left(-\frac{1}{2}\mu\tilde{\lambda}J\right)}_{\text{Exponential decay term}} + \underbrace{\frac{12\tilde{\lambda}\delta^2}{JI}}_{\text{First-order noise 1}} \\ &+ \underbrace{\frac{12\tilde{\lambda}(C-J)\nu_*^2}{J(C-1)}}_{\text{First-order noise 2}} + \underbrace{\frac{18L\tilde{\lambda}^2\delta^2}{JI}}_{\text{Second-order noise 1}} + \underbrace{\frac{18L\tilde{\lambda}^2\nu_*^2}{J}}_{\text{Second-order noise 2}}. \end{aligned}$$

The rate of convergence depends on the term that decays exponentially and the residual terms involving $\tilde{\lambda}$. The term $\exp\left(-\frac{1}{2}\mu\tilde{\lambda}J\right)$ indicates an exponential rate of convergence in J , where:

$$\exp\left(-\frac{1}{2}\mu\tilde{\lambda}J\right) \approx \mathcal{O}\left(e^{-\mu\tilde{\lambda}J/2}\right).$$

This rate is governed by the factor $\mu\tilde{\lambda}$, with a higher μ or larger $\tilde{\lambda}$ leading to faster convergence. The residual terms contribute a constant error bound determined by $\tilde{\lambda}$. In particular:

$$\frac{12\tilde{\lambda}\delta^2}{JI} + \frac{12\tilde{\lambda}(C-J)\nu_*^2}{J(C-1)} + \frac{18L\tilde{\lambda}^2\delta^2}{JI} + \frac{18L\tilde{\lambda}^2\nu_*^2}{J}.$$

These residual terms do not decay with J but are controlled by the choice of $\tilde{\lambda}$. The terms involving $\tilde{\lambda}$ and $\tilde{\lambda}^2$ suggest that setting $\tilde{\lambda}$ small enough ensures these residuals remain small.

Combining these two components, we see that: (i) Exponential decay of the error term occurs at rate $\mathcal{O}(e^{-\mu\tilde{\lambda}J/2})$, showing that the algorithm converges exponentially fast towards a neighborhood of the optimal value. (ii) The residual error is of order $\mathcal{O}(\tilde{\lambda})$ and $\mathcal{O}(\tilde{\lambda}^2)$, determined by variance-related terms.

Thus, the overall convergence rate is:

$$\mathbb{E} [F(\bar{\mathbf{x}}^{(J)}) - F(\mathbf{x}^*)] = \mathcal{O}\left(e^{-\mu\tilde{\lambda}J/2}\right) + \mathcal{O}(\tilde{\lambda}) + \mathcal{O}(\tilde{\lambda}^2),$$

where the exponential term reflects the fast convergence, and the residual terms represent the constant asymptotic error bound. \square

6. Simulations

In this section we consider the simulations setup that we employed to test our AFL algorithm by applying it for training multiple clients and single server Deep Neural Networks (DNNs) architecture for the case of climate aware wind power simulation. In the following we discuss the climate dataset, the processor unit, and detail of clients and sever model used for the simulation.

6.1. Dataset

For the dataset, in particular, we consider the CMIP6 (Coupled Model Intercomparison Project Phase 6) dataset which is a global collection of climate model outputs that provides projections of future climate change based on different greenhouse gas emission scenarios Makula and Zhou [32]. It is a key resource for researchers and policymakers to assess potential climate impacts. CMIP6 includes data from various climate models that simulate different aspects of the Earth’s climate system, such as temperature, precipitation, atmospheric pressure, and more Tebaldi et al. [33]. These models are driven by various socio-economic pathways, providing a range of possible future climate scenarios Lovato et al. [34].

In the context of our research, the CMIP6 dataset will be used to test our AFL algorithm, a decentralized machine learning approach where multiple local clients (representing different locations or regions) independently train their models on local data and periodically share model updates with a central server. This approach allows for the efficient use of distributed data, such as the global climate data from CMIP6, without the need to centralize sensitive data.

Inspired by Forootani et al. [35], we consider the CMIP6 climate dataset over Germany. The preprocessing of CMIP6 data for climate analysis and wind power simulation in Germany involves several crucial steps to ensure that the dataset is accurate, consistent, and suitable for modeling. First, spatial interpolation is performed to estimate climate variables, such as wind speed and surface pressure, at specific geographic locations. This is achieved using techniques like the Regular Grid Interpolator, which maps the data from the global climate model grid to a finer grid that corresponds to the region of interest Jung and Broadwater [36], Weiser and Zarantonello [37] ¹.

¹EE Monitor provides information on the expansion of renewable energies in Germany from an environmental perspective, <https://web.app.ufz.de/ee-monitor/>.

For CMIP6, which often uses rotated pole coordinates, coordinate transformation has to be applied to align the data with the geographic boundaries of Germany Grose et al. [38]. This ensures that the climate data accurately represents the local geography. Next, temporal interpolation is used to handle missing data or mismatched time resolutions, as CMIP6 datasets typically have a 3-hour temporal resolution, while wind power data often is recorded at an hourly resolution ². To harmonize these datasets, resampling and aggregation methods are applied, converting the data into standard time intervals, such as 3-hour periods, to ensure consistency across all datasets. Finally, filtering based on latitude and longitude coordinates helps to focus on the region of interest, narrowing the dataset to only include data relevant to Germany. These preprocessing steps facilitate the integration of CMIP6 data into wind power forecasting models and other atmospheric analyses, ensuring high-quality input for renewable energy research and decision-making. For more details we refer the reader to the original work of the authors reported in Forootani et al. [35].

6.2. Code and data availability statement

The AFL framework is implemented using the PyTorch framework, leveraging its advanced tools for model construction and optimization. The code for this federated learning approach, including the client selection, delay tracking, and model aggregation mechanisms, is openly available to support reproducibility and further research in decentralized machine learning and federated optimization. The implementation, including detailed comments and instructions for reproducing the results, is hosted in the associated GitHub repository ³. The repository provides code for the asynchronous training loop, model aggregation, delay-aware optimization, and evaluation of the global model. Additionally, a version of the code will be archived on Zenodo⁴ for reference.

Hardware. Our machine is powered by a 13th Gen Intel[®] Core[™] i5-1335U processor with 10 cores, 12 threads, and a maximum clock speed of 4.6 GHz.

²see e.g. <https://open-power-system-data.org/>

³<https://github.com/Ali-Forootani/Asynchronous-Federated-Learning>

⁴<https://zenodo.org/records/14548841>, DOI: 10.5281/zenodo.14548841

6.3. Clients and Server Models

Without loss of generality to test the proposed AFL algorithm, we consider to enable multiple clients to collaboratively train a shared Long Short Term Memory (LSTM)-based deep learning model while keeping their data local. LSTMs are particularly suitable for time-series forecasting tasks, such as wind power generation, due to their ability to capture temporal dependencies in sequential data. Each client in the AFL setup has its own LSTM-based deep learning model and associated training components.

Clients model. The clients have the following settings: (i) Each client uses a multi-layer deep recurrent neural network based on LSTM units; (ii) The model architecture consists of multiple LSTM layers (stacked sequentially) followed by a fully connected layer to predict the target output; (iii) The training loss is calculated using the Mean Squared Error (MSE) function, which is strongly convex function as we assumed the local objective functions; (iv) Each client trains its local model for a fixed number of epochs using its own dataset. Training updates are derived from the gradients of the local loss function with respect to the model parameters.

Server model. The server in AFL acts as a central coordinator that aggregates updates from all client models and maintains a global version of the model. The server has the following settings: (i) The server initializes a global model, structurally identical to the client models, which serves as the shared model for all clients; (ii) After each round of local training, the global model parameters are updated based on the aggregated updates from the client models; (iii) The server uses a specified aggregation method (e.g., average or weighted average) to combine the model parameters or gradients from the clients.

The approach leverages asynchronous updates, client selection strategies, and delay-aware optimization to improve the performance and efficiency of federated training under diverse real-world conditions.

Client Training with Strong Convexity and Time Delays. The client training function incorporates a dynamic learning rate governed by strong convexity principles, expressed as $\gamma_i = \frac{\gamma_0}{\sqrt{i+1}(1+\alpha\cdot\tau_i)}$. This formulation adapts the learning rate based on the epoch number and observed delays, ensuring stable convergence despite heterogeneous client conditions. Clients use an Adam optimizer for gradient updates, with gradient scaling enabled through mixed-precision training (AMP) for computational efficiency.

Time delays experienced by clients are explicitly modeled and tracked during each round, enabling a delay-aware adjustment to learning rates. This mechanism addresses the common issue of stragglers in federated learning, where delays from slower devices can hinder the training process. By incorporating delays into the learning rate calculation, the algorithm improves resilience to heterogeneity in client hardware and network conditions.

Client Selection and Fairness. To ensure fair participation among clients, the training loop uses a balanced client selection strategy. Clients are sampled without replacement within each round, with mechanisms in place to maintain diversity across rounds. This approach mitigates potential biases in the aggregation process and promotes equitable contributions from all clients over time.

The number of clients participating in each round is randomized within predefined bounds, providing additional robustness against overfitting to specific subsets of data. This stochastic element enhances the generalization capabilities of the global model.

Weighted Aggregation of Client Updates. The aggregation of client updates is implemented using a weighted averaging scheme, where the weight of each client’s contribution is proportional to its dataset size. This ensures that updates from clients with larger datasets have a more significant impact on the global model, aligning the optimization process with the distribution of data across clients. The algorithm initializes an empty server state dictionary and iteratively accumulates weighted updates from all participating clients, thereby producing an aggregated global model.

Asynchronous Training with Delay Tracking. The asynchronous nature of the algorithm is supported by Python’s `asyncio` module, which allows clients to train independently and in parallel. This design improves the utilization of computational resources and reduces overall training time by avoiding bottlenecks caused by slower clients. Time delays for each client are tracked and analyzed, with metrics such as the maximum delay per round being reported. These insights provide valuable feedback for optimizing the training process and .

Early Stopping for Efficiency. To prevent unnecessary computations, an early stopping mechanism is employed at the client level. Clients terminate training if the validation loss does not improve for a specified number of epochs,

reducing computational overhead and accelerating the training process. This feature is particularly useful in resource-constrained environments where computational power and energy consumption are critical concerns.

Evaluation and Dynamic Scheduling. The server model is evaluated after each round using data from all clients, ensuring consistent monitoring of global performance. The training loop also incorporates a dynamic learning rate scheduler (Cosine Annealing) to adjust the server model’s learning rate over time, which aids in fine-tuning the global model during later stages of training.

6.4. Numerical results

DNN structure of each client takes 5 inputs based on the climate dataset including (i) time, (ii) Latitude coordinate, (iii) Longitude coordinate, (iv) wind speed and (v) pressure surface; while it has one output which is wind power production.

Each client has LSTM model architecture which contains 3 stacked LSTM layers and each LSTM layer consists of 32 hidden units. The LSTM layers internally handle gate activations (input, forget, output) for processing time-series data. Moreover, the output from the final LSTM layer is passed through a fully connected layer to generate predictions. Finally, a single dense layer maps the final LSTM hidden state to the predicted output with a size of 1. The server model is identical to local clients. In the training loop each client trains its local LSTM model using its portion of the dataset, optimizing weights using stochastic gradient descent. After local training, each participating client shares its model weights with the server. The server aggregates the weights using the weighted average method to update the global model.

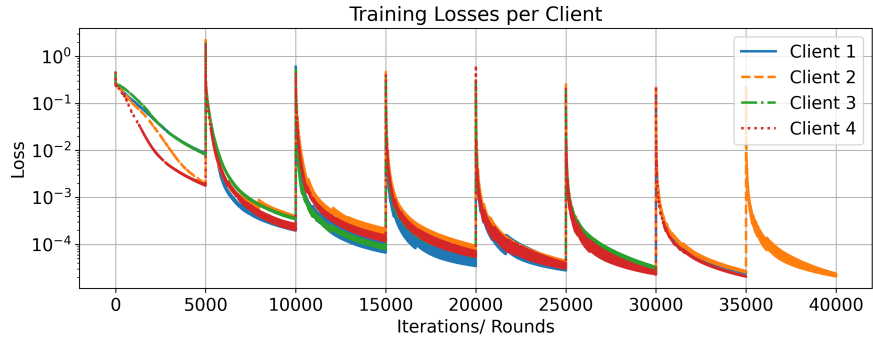
Scenario I. For the first simulation we consider total number of $C = 4$ clients and the data is partitioned among them for training ensuring data privacy; A maximum possible subset of clients, defined by $J = 4$ participates in each training round which will be chosen randomly at each round; number of rounds $\mathcal{J} = 10$ which means AFL process is conducted over 10 rounds of communication between the clients and the server; local training epochs $I = 5,000$ which means each client trains its local model for 5,000 epochs before sharing updates with the server; dynamical learning rate with parameters $\gamma_0 = 0.01$, $\alpha = 0.001$; early stopping patience iterations is 2000 which

means training will stop early if no improvement is observed for 2000 epochs, preventing overfitting or unnecessary computations. Moreover client updates are aggregated using a weighted averaging scheme to produce the global model.

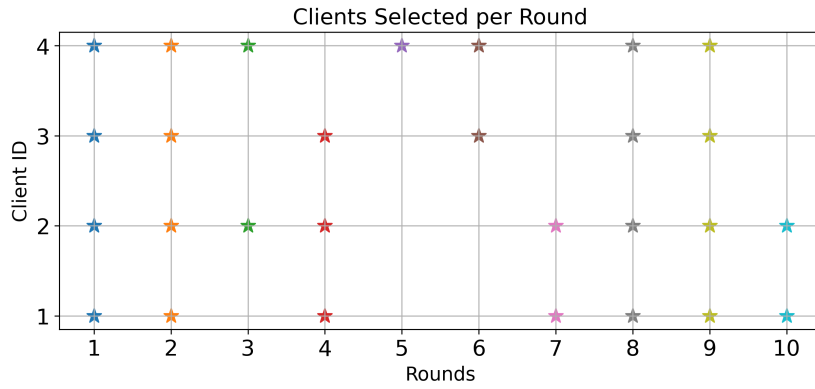
The updated global model is redistributed to the clients, and this process is repeated for $\mathcal{J} = 10$ iterations. Figure 1a illustrates the training loss for each client over the total number of iterations. As observed, the training loss decreases progressively with an increase in the number of iterations during each round. Figure 1b shows the clients selected for training in each round. Notably, client 2 is chosen more frequently than the other clients. This is also evident in Figure 1a, where its training loss corresponds to $8 \times 5000 = 40000$ total iterations. Figure 1c depicts the maximum delay for each round, showing that the delay is proportional to the number of clients participating in training during a given round. For example, rounds 2, 8, and 9 exhibit the highest delays, whereas round 5 experiences no delay since only one client participates in training. It is worth emphasizing that the execution time and delay are strongly influenced by the computational capabilities of the processor used in the AFL algorithm.

Scenario II. In the second scenario, similar to the first, a total of $C = 4$ clients are considered. However, the maximum number of clients allowed to participate in training at any given time is limited to $J = 3$. The training loss for each client is shown in Figure 2a, where we observe the convergence of the client’s losses over the training iterations. The participation of each client is depicted in Figure 2b, with client 3 having the highest participation, appearing in a total of 6 rounds. Figure 2c illustrates the maximum delay during each round, demonstrating that the delay increases with the number of active clients participating simultaneously. For instance, rounds 1, 2, and 9 experience the maximum delay, as all 3 clients are active in training during these rounds.

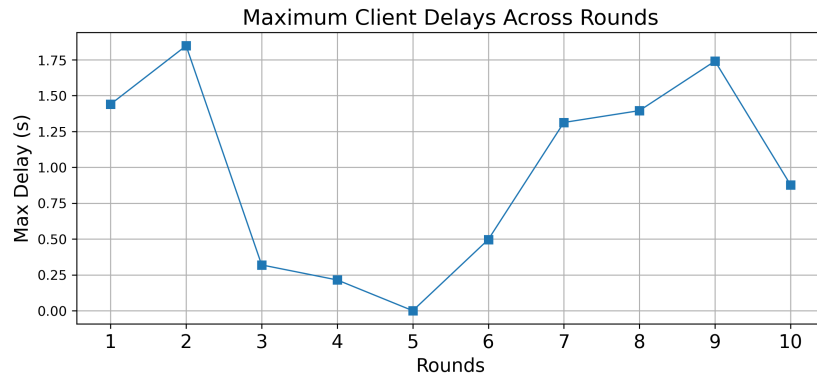
Scenario III. In the third scenario, we consider a total of $C = 5$ clients with a maximum client participation of $J = 5$. The training loss is shown in Figure 3a, illustrating the convergence of the training losses for each client over the training iterations. Figure 3b displays the clients selected in each round of training, where clients 1 and 2 participate most frequently, with a maximum of 6 rounds. The figure also highlights that the largest delays occur when 3 or 4 clients participate in each training round. This observation indicates



(a) Clients losses through the training loops for the case of total number of $C = 4$ clients and maximum client participation in training $J = 4$.

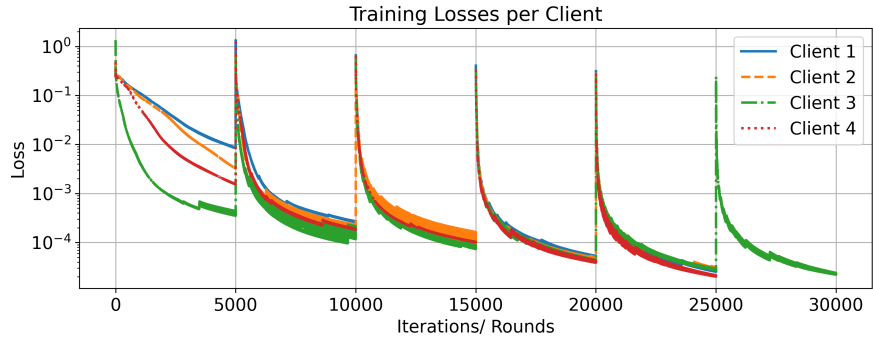


(b) Selected clients for each round with maximum client's participation $J = 4$.

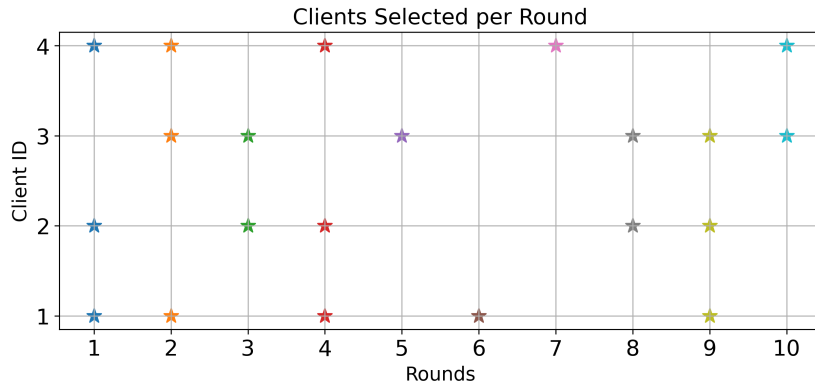


(c) Maximum delays among clients for the case of total number of $C = 4$ clients and maximum client participation in training loop $J = 4$.

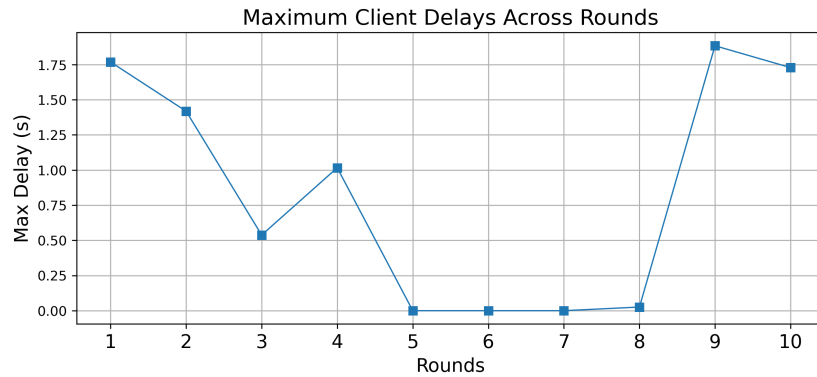
Figure 1: AFL performance in training of the LSTM based DNN client's models with total number of $C = 4$ clients and maximum participation of $J = 3$ clients per each round



(a) Clients losses through the training loops for the case of total number of $C = 4$ clients and maximum client participation in training $J = 3$.



(b) Selected clients for each round with maximum client's participation $J = 3$.



(c) Maximum delays among clients for the case of total number of $C = 4$ clients and maximum client participation in training loop $J = 3$.

Figure 2: AFL performance in training of the LSTM based DNN client's models with total number of $C = 4$ clients and maximum participation of $J = 3$ clients per each round

that, for a fixed dataset size, distributing the data among more clients during training rounds reduces the drift between clients.

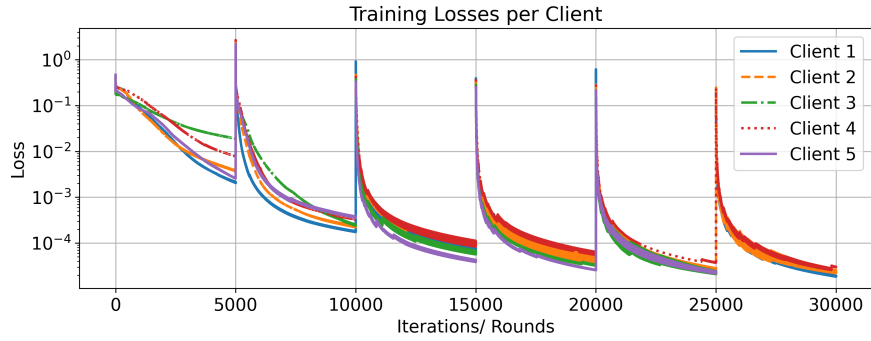
Scenario IV. In the fourth scenario, we examine a more practical case involving a total of $C = 6$ clients, with a maximum participation of $J = 4$ clients per training round, over a total of $\mathcal{J} = 50$ rounds, each consisting of $I = 1000$ iterations. The training losses exhibit behavior similar to the previous examples. However, the client delays are significantly influenced by the total number of clients (C), the total number of rounds (\mathcal{J}), and the number of clients participating in each round of training (see Figure 4c).

7. Conclusion

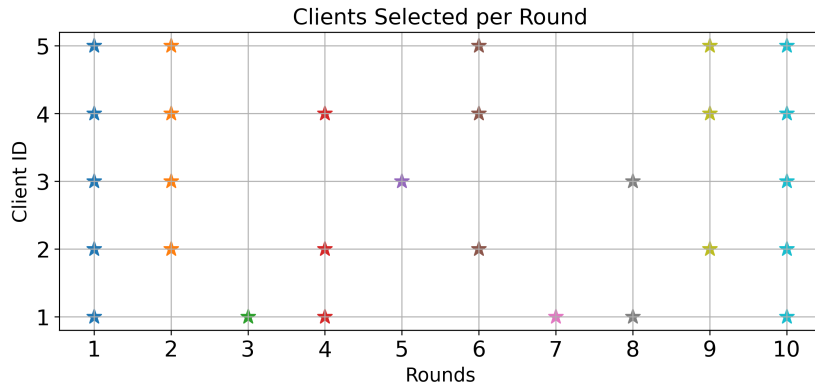
In this paper we proposed AFL algorithm that significantly improved the scalability, efficiency, and robustness of federated learning systems, especially in scenarios involving heterogeneous client populations and dynamic network conditions. By allowing clients to update the global model asynchronously, AFL mitigated the inefficiencies and delays associated with synchronous methods, leading to faster convergence and better resource utilization. Our theoretical analysis, supported by variance bounds and martingale difference sequence theory, demonstrates that AFL can effectively handle client delays and model staleness, ensuring reliable convergence even in challenging environments. The practical applicability of AFL is further validated through the successful training of a decentralized LSTM model on the CMIP6 climate dataset, highlighting its potential for large-scale, privacy-preserving applications in diverse, real-world settings. This work paves the way for more efficient distributed learning frameworks, particularly in resource-constrained and dynamically changing environments.

The simulations demonstrated the effectiveness of the proposed AFL algorithm for training a decentralized DNN using CMIP6 climate data for wind power forecasting. The algorithm successfully leverages an asynchronous federated learning framework to enable multiple clients to train local models independently while collaborating through a central server. Key features such as dynamic learning rate adjustment, delay-aware optimization, weighted aggregation, and early stopping ensure robust and efficient training across heterogeneous clients with diverse data distributions.

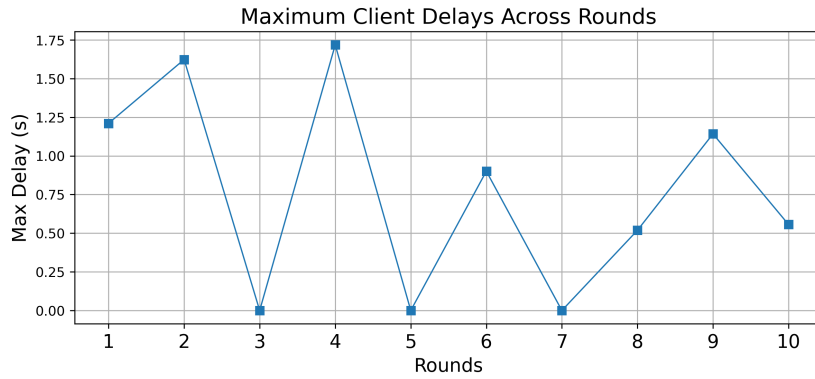
The results highlighted the adaptability of the AFL algorithm to various configurations, as evidenced by its ability to reduce training loss over iterations and maintain fairness in client participation. The use of LSTM-based



(a) Clients losses throughout training for the case of maximum number of clients $C = 5$ and maximum client participation in training $J = 5$.

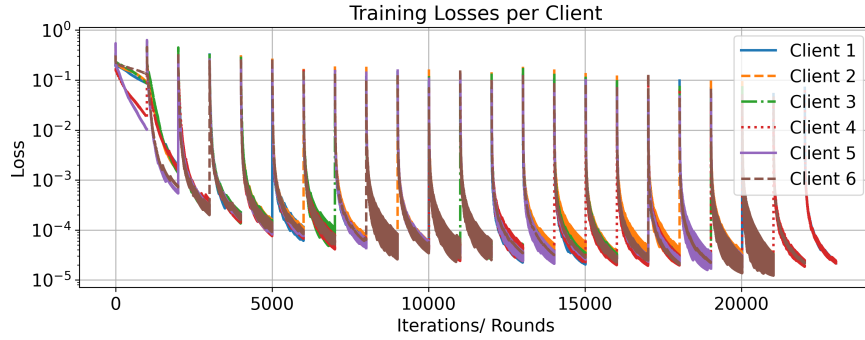


(b) Selected clients for each round with maximum client participation $J = 5$

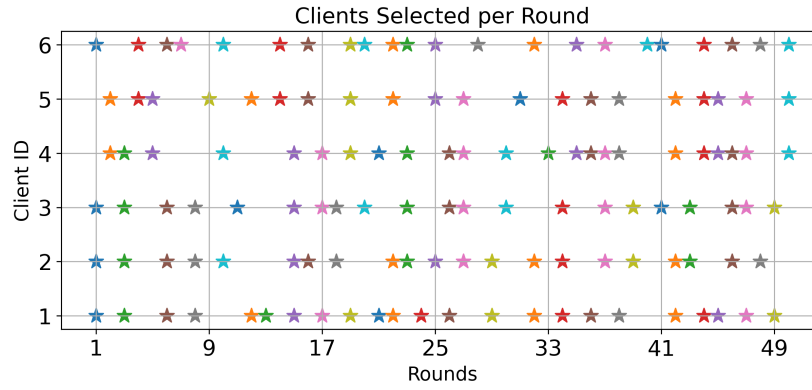


(c) Max delays among the clients for each round

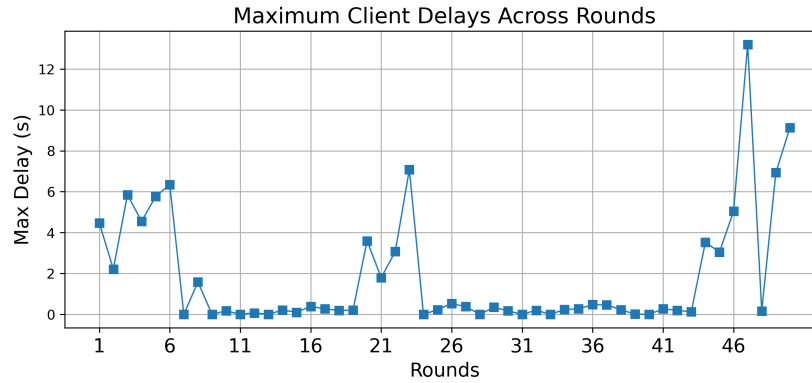
Figure 3: AFL performance in training of the LSTM based DNN client's models with total number of $C = 5$ clients and maximum participation of $J = 5$ clients per each round



(a) Clients losses throughout the training for the case of maximum number of clients $C = 6$ and maximum client participation in training $J = 4$.



(b) Selected clients for each round with maximum client participation $J = 4$



(c) Max delays among the clients for each round

Figure 4: AFL performance in training of the LSTM based DNN client's models with total number of $C = 6$ clients and maximum participation of $J = 4$ clients per each round

architectures further validates the suitability of this approach for time-series forecasting tasks in renewable energy research. Scenario-based evaluations confirm the algorithm’s scalability and capability to address real-world challenges such as non-uniform client contributions and variable training conditions.

The AFL algorithm represents a significant advancement in decentralized machine learning, with promising real-life applications across various domains, such as climate-aware energy modeling, smart grids Jithish et al. [39], distributed healthcare systems Nguyen et al. [40], intelligent transportation networks Posner et al. [41], and physics informed neural networks Forootani and Benner [42], Forootani et al. [43, 44]. These applications benefit from asynchronous federated learning by enabling robust model training while addressing critical challenges such as data privacy, uneven computational resources, and communication efficiency. By leveraging its capacity for asynchronous updates, AFL facilitates real-time adaptability and efficient resource utilization, making it particularly suited for dynamic environments and large-scale deployments.

For the future work we plan to involve exploring larger-scale simulations, convergence analysis of AFL algorithm for the case of general convex and non-convex local objective functions for physics informed neural network problems.

8. Appendix

To simplify the expression, we define:

$$\Gamma = \sum_{c=1}^J \sum_{i=0}^{I-1} \mathbb{E} \left[\left\| \sum_{i=1}^c \sum_{j=0}^{p_{c,i}(i)} (\mathbf{x}_{\psi_i} - \bar{\mathbf{x}}) \right\|^2 \right].$$

We start by expanding Γ :

$$\begin{aligned} \Gamma &= \frac{CI^3\nu^2}{C-1} \sum_{c=1}^J (c-1) - \frac{I^3\nu^2}{C-1} \sum_{c=1}^J (c-1)^2 \\ &\quad + J\nu^2 \sum_{i=0}^{I-1} i^2 - \frac{2I\nu^2}{C-1} \sum_{c=1}^J (c-1) \sum_{i=0}^{I-1} i. \end{aligned}$$

Substituting the known summation formulas, we have:

$$\Gamma = \frac{CI^3}{C-1} \frac{(J-1)J}{2} - \frac{I^3}{J-1} \frac{(J-1)J(2J-1)}{6} + J \frac{(I-1)I(2I-1)}{6} - \frac{2I}{J-1} \frac{(J-1)J(I-1)I}{2}.$$

Next, we separate the first term into two components:

$$\Gamma = \frac{(J-1)JI^3}{2} + \frac{I^3}{C-1} \frac{(J-1)J}{2} - \frac{I^3}{C-1} \frac{(J-1)J(2J-1)}{6} + C \frac{(I-1)I(2I-1)}{6} - \frac{2I}{C-1} \frac{(J-1)J(I-1)I}{2}.$$

Next, we group the terms containing $\frac{1}{C-1}$:

$$\Gamma = \frac{(J-1)JI^3}{2} + J \frac{(I-1)I(2I-1)}{6} + \frac{I^3}{C-1} \frac{(J-1)J}{2} - \frac{I^3}{C-1} \frac{(J-1)J(2J-1)}{6} - \frac{2I}{C-1} \frac{(J-1)J(I-1)I}{2}. \quad (38)$$

Now, we analyze the first two terms in (38):

$$\begin{aligned} \text{Term}_1 + \text{Term}_2 &= \frac{J^2 I^3}{2} - JI \left(\frac{3I^2}{6} - \frac{(I-1)(2I-1)}{6} \right) \\ &= \frac{J^2 I^3}{2} - \frac{JI(I^2 + 3I - 1)}{6} = \frac{1}{2} JI^2(JI - 1) - \frac{1}{6} JI(I^2 - 1). \end{aligned}$$

Next, we consider the remaining three terms in (38):

$$\text{Term}_3 + \text{Term}_4 + \text{Term}_5 = \frac{I^2}{C-1} \left(\frac{(J-1)JI}{2} - \frac{(J-1)J(2J-1)I}{6} - \frac{(J-1)J(I-1)}{2} \right). \quad (39)$$

Rearranging (39) gives:

$$\begin{aligned} \text{Term}_3 + \text{Term}_4 + \text{Term}_5 &= -\frac{I^2}{C-1} \left(\frac{(J-1)J(2J-1)I}{6} - \frac{(J-1)J}{2} \right) \\ &= -\frac{(J-1)JI^2}{2(C-1)} \left(\frac{1}{3}(2J-1)I - 1 \right). \end{aligned}$$

Finally, we can summarize our results to obtain:

$$\Gamma = \frac{1}{2}JI^2(JI - 1) - \frac{1}{6}JI(I^2 - 1) - \frac{1}{2} \frac{(J - 1)J}{(C - 1)} I^2 \left(\frac{1}{3}(2J - 1)I - 1 \right), \quad (40)$$

comparing (40) with the right hand side of (18) the results .

9. Biography

Ali Forootani received the M.Sc. degree in electrical engineering and automatic control systems from the Power and Water University of Technology (Iran) in 2011, and the Ph.D. degree from the Department of Engineering, University of Sannio (Italy) in 2019. From 2011 to 2015 he worked both on research and industry at Niroo Research Institute (Iran) and at the Ministry of Energy and Power (Iran). From 2019 to 2024, he served as a Postdoctoral researcher at the University of Sannio, the University of Salerno, at Maynooth University (Ireland), and the Max Planck Institute for Dynamics of Complex Technical Systems in Magdeburg (Germany). Since May 2024, he has been affiliated with the Helmholtz Center for Environmental Research-UFZ in Leipzig (Germany). His current research interests include Markov decision processes, Approximate Dynamic Programming, Reinforcement Learning in optimal control, network control systems, Physics Informed Neural Networks (PINNs), PDE parameter estimation and identification, Federated Learning, and Large Language Models. He is a Senior Member of IEEE Control System Society.

References

- [1] L. Li, Y. Fan, M. Tse, K.-Y. Lin, A review of applications in federated learning, *Computers & Industrial Engineering* 149 (2020) 106854.
- [2] C. Zhang, Y. Xie, H. Bai, B. Yu, W. Li, Y. Gao, A survey on federated learning, *Knowledge-Based Systems* 216 (2021) 106775.
- [3] R. S. Antunes, C. André da Costa, A. Küderle, I. A. Yari, B. Eskofier, Federated learning for healthcare: Systematic review and architecture proposal, *ACM Transactions on Intelligent Systems and Technology (TIST)* 13 (2022) 1–23.

- [4] J. Wen, Z. Zhang, Y. Lan, Z. Cui, J. Cai, W. Zhang, A survey on federated learning: challenges and applications, *International Journal of Machine Learning and Cybernetics* 14 (2023) 513–535.
- [5] D. C. Nguyen, M. Ding, P. N. Pathirana, A. Seneviratne, J. Li, H. V. Poor, Federated learning for internet of things: A comprehensive survey, *IEEE Communications Surveys & Tutorials* 23 (2021) 1622–1658.
- [6] B. McMahan, E. Moore, D. Ramage, S. Hampson, B. A. y Arcas, Communication-efficient learning of deep networks from decentralized data, in: *Artificial intelligence and statistics*, PMLR, 2017, pp. 1273–1282.
- [7] K. Chang, N. Balachandar, C. Lam, D. Yi, J. Brown, A. Beers, B. Rosen, D. L. Rubin, J. Kalpathy-Cramer, Distributed deep learning networks among institutions for medical imaging, *Journal of the American Medical Informatics Association* 25 (2018) 945–954.
- [8] S. P. Karimireddy, S. Kale, M. Mohri, S. Reddi, S. Stich, A. T. Suresh, Scaffold: Stochastic controlled averaging for federated learning, in: *International Conference on Machine Learning*, PMLR, 2020, pp. 5132–5143.
- [9] X. Li, K. Huang, W. Yang, S. Wang, Z. Zhang, On the convergence of fedavg on non-iid data, in: *International Conference on Learning Representations*, 2019.
- [10] A. Khaled, K. Mishchenko, P. Richtárik, Tighter theory for local sgd on identical and heterogeneous data, in: *International Conference on Artificial Intelligence and Statistics*, PMLR, 2020, pp. 4519–4529.
- [11] A. Koloskova, N. Loizou, S. Boreiri, M. Jaggi, S. Stich, A unified theory of decentralized sgd with changing topology and local updates, in: *International Conference on Machine Learning*, PMLR, 2020, pp. 5381–5393.
- [12] B. E. Woodworth, K. K. Patel, N. Srebro, Minibatch vs local sgd for heterogeneous distributed learning, *Advances in Neural Information Processing Systems* 33 (2020) 6281–6292.

- [13] J. Wang, Q. Liu, H. Liang, G. Joshi, H. V. Poor, Tackling the objective inconsistency problem in heterogeneous federated optimization, *Advances in neural information processing systems* 33 (2020) 7611–7623.
- [14] H. Yang, M. Fang, J. Liu, Achieving linear speedup with partial worker participation in non-IID federated learning, in: *International Conference on Learning Representations*, 2021. URL: <https://openreview.net/forum?id=jDdzh5ul-d>.
- [15] S. Wang, M. Ji, A unified analysis of federated learning with arbitrary client participation, *Advances in Neural Information Processing Systems* 35 (2022) 19124–19137.
- [16] S. J. Reddi, Z. Charles, M. Zaheer, Z. Garrett, K. Rush, J. Konečný, S. Kumar, H. B. McMahan, Adaptive federated optimization, in: *International Conference on Learning Representations*, 2021. URL: <https://openreview.net/forum?id=LkFG31B13U5>.
- [17] M. Gürbüzbalaban, A. Ozdaglar, P. A. Parrilo, Why random reshuffling beats stochastic gradient descent, *Mathematical Programming* 186 (2021) 49–84.
- [18] J. Haochen, S. Sra, Random shuffling beats sgd after finite epochs, in: *International Conference on Machine Learning*, PMLR, 2019, pp. 2624–2633.
- [19] D. Nagaraj, P. Jain, P. Netrapalli, Sgd without replacement: Sharper rates for general smooth convex functions, in: *International Conference on Machine Learning*, PMLR, 2019, pp. 4703–4711.
- [20] K. Ahn, C. Yun, S. Sra, Sgd with shuffling: optimal rates without component convexity and large epoch requirements, *Advances in Neural Information Processing Systems* 33 (2020) 17526–17535.
- [21] K. Mishchenko, A. Khaled, P. Richtárik, Random reshuffling: Simple analysis with vast improvements, *Advances in Neural Information Processing Systems* 33 (2020) 17309–17320.
- [22] I. Safran, O. Shamir, How good is sgd with random shuffling?, in: *Conference on Learning Theory*, PMLR, 2020, pp. 3250–3284.

- [23] I. Safran, O. Shamir, Random shuffling beats sgd only after many epochs on ill-conditioned problems, *Advances in Neural Information Processing Systems* 34 (2021) 15151–15161.
- [24] S. Rajput, A. Gupta, D. Papailiopoulos, Closing the convergence gap of sgd without replacement, in: *International Conference on Machine Learning*, PMLR, 2020, pp. 7964–7973.
- [25] J. Cha, J. Lee, C. Yun, Tighter lower bounds for shuffling sgd: Random permutations and beyond, *arXiv preprint arXiv:2303.07160* (2023).
- [26] K. Mishchenko, A. Khaled, P. Richtárik, Proximal and federated random reshuffling, in: *International Conference on Machine Learning*, PMLR, 2022, pp. 15718–15749.
- [27] C. Yun, S. Rajput, S. Sra, Minibatch vs local SGD with shuffling: Tight convergence bounds and beyond, in: *International Conference on Learning Representations*, 2022. URL: <https://openreview.net/forum?id=LdlwbBP2mlq>.
- [28] Y. J. Cho, P. Sharma, G. Joshi, Z. Xu, S. Kale, T. Zhang, On the convergence of federated averaging with cyclic client participation, *arXiv preprint arXiv:2302.03109* (2023).
- [29] Y. Chen, Y. Ning, M. Slawski, H. Rangwala, Asynchronous online federated learning for edge devices with non-iid data, in: *2020 IEEE International Conference on Big Data (Big Data)*, IEEE, 2020, pp. 15–24.
- [30] L. Leconte, M. Jonckheere, S. Samsonov, E. Moulines, Queuing dynamics of asynchronous federated learning, in: *International Conference on Artificial Intelligence and Statistics*, PMLR, 2024, pp. 1711–1719.
- [31] S. Boyd, L. Vandenberghe, *Convex optimization*, Cambridge university press, 2004.
- [32] E. K. Makula, B. Zhou, Coupled model intercomparison project phase 6 evaluation and projection of east african precipitation, *International Journal of Climatology* 42 (2022) 2398–2412.

- [33] C. Tebaldi, K. Debeire, V. Eyring, E. Fischer, J. Fyfe, P. Friedlingstein, R. Knutti, J. Lowe, B. O’Neill, B. Sanderson, et al., Climate model projections from the scenario model intercomparison project (scenariomip) of cmip6, *Earth System Dynamics* 12 (2021) 253–293.
- [34] T. Lovato, D. Peano, M. Butenschön, S. Materia, D. Iovino, E. Scocimarro, P. Fogli, A. Cherchi, A. Bellucci, S. Gualdi, et al., C mip6 simulations with the cmcc earth system model (cmcc-esm2), *Journal of Advances in Modeling Earth Systems* 14 (2022) e2021MS002814.
- [35] A. Forootani, D. Esmaeili Aliabadi, D. Thrän, Climate aware deep neural networks (CADNN) for wind power simulation, *arXiv:2412.12160* (2024).
- [36] J. Jung, R. P. Broadwater, Current status and future advances for wind speed and power forecasting, *Renewable and Sustainable Energy Reviews* 31 (2014) 762–777.
- [37] A. Weiser, S. E. Zarantonello, A note on piecewise linear and multilinear table interpolation in many dimensions, *Mathematics of Computation* 50 (1988) 189–196.
- [38] M. R. Grose, S. Narsey, R. Trancoso, C. Mackallah, F. Delage, A. Dowdy, G. Di Virgilio, I. Watterson, P. Dobrohotoff, H. A. Rashid, et al., A cmip6-based multi-model downscaling ensemble to underpin climate change services in australia, *Climate Services* 30 (2023) 100368.
- [39] J. Jithish, B. Alangot, N. Mahalingam, K. S. Yeo, Distributed anomaly detection in smart grids: a federated learning-based approach, *IEEE Access* 11 (2023) 7157–7179.
- [40] D. C. Nguyen, Q.-V. Pham, P. N. Pathirana, M. Ding, A. Seneviratne, Z. Lin, O. Dobre, W.-J. Hwang, Federated learning for smart healthcare: A survey, *ACM Computing Surveys (Csur)* 55 (2022) 1–37.
- [41] J. Posner, L. Tseng, M. Aloqaily, Y. Jararweh, Federated learning in vehicular networks: Opportunities and solutions, *IEEE Network* 35 (2021) 152–159.

- [42] A. Forootani, P. Benner, GN-SINDy: Greedy sampling neural network in sparse identification of nonlinear partial differential equations, arXiv preprint arXiv:2405.08613 (2024).
- [43] A. Forootani, H. Kapadia, S. Chellappa, P. Goyal, P. Benner, GS-PINN: Greedy sampling for parameter estimation in partial differential equations, arXiv preprint arXiv:2405.08537 (2024).
- [44] A. Forootani, P. Goyal, P. Benner, A robust SINDy approach by combining neural networks and an integral form, arXiv preprint arXiv:2309.07193 (2023).